

7-2008

REMChlor Model of Tritium Transport at the MADE Site

Shelly Tyre

Clemson University, shejaty@gmail.com

Follow this and additional works at: https://tigerprints.clemson.edu/all_theses

 Part of the [Environmental Sciences Commons](#)

Recommended Citation

Tyre, Shelly, "REMChlor Model of Tritium Transport at the MADE Site" (2008). *All Theses*. 415.

https://tigerprints.clemson.edu/all_theses/415

This Thesis is brought to you for free and open access by the Theses at TigerPrints. It has been accepted for inclusion in All Theses by an authorized administrator of TigerPrints. For more information, please contact kokeefe@clemson.edu.

REMCHLOR MODEL OF TRITIUM TRANSPORT
AT THE MADE SITE

A Thesis
Presented to
the Graduate School of
Clemson University

In Partial Fulfillment
of the Requirements for the Degree
Master of Science
Hydrogeology

by
Shelly J. Tyre
August 2008

Accepted by:
Dr. Ron W. Falta, Committee Chair
Dr. Fred Molz
Dr. Stephen Moysey

ABSTRACT

Groundwater transport models are commonly used at sites with groundwater contamination. Models are used to study the extent of the contamination and the possible risks it poses. Contaminant transport models use properties of the aquifer and the solute to simulate how the solute moves through the aquifer. Screening level models are often used as a first modeling approach at sites to get an idea of the general trends of contaminant transport. They offer an efficient approach to modeling, usually requiring fewer input parameters than other models.

This study uses a screening level model to describe tritium transport for the second Macro-Dispersion Experiment (MADE). The MADE site, at Columbus Air Force Base, Mississippi, is situated at an aquifer with a high degree of heterogeneity in hydraulic conductivity. The variability in hydraulic conductivity at the site produces non-classical tritium transport. Ideally, the tritium tracer should have behaved as an instantaneous source with a tracer pulse traveling with groundwater flow. However, the actual distribution of tritium by the end of the sampling period shows that the bulk of the tracer stays within 20 m of the injection site with a low-concentration leading edge extending almost 300 m downgradient.

There have been a variety of attempts to model the tritium distribution for the MADE-2 experiment. A traditional advection-dispersion model with an instantaneous point-source fails to capture the actual tritium distribution. Others have used dual-domain mass transfer numerical models to capture the tritium distribution.

An alternate approach is to treat the area near the injection site as a source zone, where the discharge concentration leaving the source is proportional to the tritium mass remaining in this zone. This study uses REMChlor, an analytical model available through the US EPA. REMChlor uses a source-plume concept to describe solute transport at sites that have non-aqueous phase liquid (NAPL) contamination.

REMChlor was used for this modeling approach with the source depletion term set to 1 ($\Gamma = 1$) to simulate exponential depletion of the mass in the source zone. This produces a 1 to 1 relationship between source mass and discharge. The ability of this model to reproduce the tritium distributions is largely dependent on the size of the area defined as the source zone. This approach reproduces key features of the observed tritium distributions such as the plume length and the mass distribution along the centerline of the site.

DEDICATION

I am dedicating this thesis to my parents who are always there for me with support and encouragement. I am grateful to them for sharing with me their passion for learning and for teaching me the value of perseverance.

ACKNOWLEDGEMENTS

I would like to thank Dr. Ron Falta, my advisor, for the opportunity to work with him. I appreciate all of his help and am very thankful for his patience. I also thank Dr. Fred Molz, Dr. Stephen Moysey, and Dr. Larry Murdoch for their input and comments and for taking the time to review my thesis. I also want to thank Jianyong Guan for her help and cooperation.

TABLE OF CONTENTS

	Page
TITLE PAGE	i
ABSTRACT	ii
DEDICATION	iv
ACKNOWLEDGEMENTS	v
LIST OF TABLES	viii
LIST OF FIGURES	ix
CHAPTER	
1. INTRODUCTION	1
1.1 Solute Transport in Groundwater.....	1
1.2 Screening Level Models.....	3
1.3 Tritium Tracer Experiments.....	5
1.4 Objectives.....	6
2. MADE SITE ANALYSIS.....	7
2.1 Site Characterization	7
2.1.1 Geologic Description	7
2.1.2 Hydrologic Setting.....	9
2.2 Tracer Experiment.....	15
2.2.1 Tritium Tracer Experiment Setup	15
2.2.2 Tritium Distribution	16
3. PREVIOUS STUDIES.....	22
3.1 Spatial Moments Analysis.....	22
3.2 Single-Domain Advection-Dispersion Models	26
3.3 Dual-Domain Mass Transfer Models.....	28
4. REMCHLOR	31
4.1 Mathematical Model	31
4.1.1 Source Model	32

Table of Contents (continued)

	Page
4.1.2 Plume Model.....	37
5. REMCHLOR SIMULATIONS	42
5.1 Classical transport.....	42
5.1.1 Source Zone	43
5.1.2 Plume Zone	47
5.1.3 Results.....	49
5.1.4 Mass Distributions	52
5.2 Souce – Plume Model	58
5.2.1 Parameters.....	58
5.2.2 Mass Distributions	63
5.2.3 Concentration Distributions	67
5.3 Discussion	70
5.4 Implications.....	72
6. CONCLUSIONS.....	77
REFERENCES	79

LIST OF TABLES

Table	Page
2.1. MADE-2 tracer test parameters	15
3.1. Results of the spatial moment analysis at each snapshot (Boggs et al., 1993).	23
3.2. Velocity values for the time period leading up to each snapshot. Calculated from center of mass estimates.	25
5.1. The maximum distance reached by the leading edge of the plume at each sampling snapshot. The velocity of the leading edge was calculated for the time leading up to each time step.....	48
5.2. Input parameters used to simulate classical tritium transport.	50
5.3. The range along the longitudinal (x) axis covered by each zone for the mass distribution plots.	52
5.4. Parameters used to simulate tritium transport at the MADE-2 site.	62

LIST OF FIGURES

Figure	Page
2.1 MADE site location. (Boggs et al., 1990).....	8
2.2 Variations in water table elevation between June 1990 and September 1991 in well p54 at 2 depths: shallow (p54a) and deep (p54b). (Guan, 2006).....	10
2.3. Hydraulic conductivity along the centerline. (Boggs et al., 1993)	12
2.4. Depth-averaged hydraulic conductivity profile. (Boggs et al., 1993).....	13
2.5. Maps of the potentiometric surface for June 1990 head measurements. (Boggs et al., 1993).	14
2.6. Sampling network. (Boggs et al., 1993).	17
2.7. Tritium concentrations at an elevation of 59 m for the 4 snapshots.	19
2.8. Tritium distributions along the centerline of the plume.....	20
2.9. Tritium distribution at 328 days (top) compared with hydraulic conductivity distribution (bottom, Boggs et al., 1993) along the centerline of the site.....	21
3.1. Longitudinal center of mass displacement for 4 snapshots. (Data from Boggs et al 1993).....	26
3.2. Concept behind DDMT models. The aquifer is divided into a mobile and immobile domain with mass transfer between each zone.	28
4.1. Conceptual model of coupled source and plume zones. (Modified from Falta et al., 2007.).....	32
4.2. Plots of the source power function for varying values of Γ	34
4.3. Conceptual model of instantaneous transport in REMChlor, where $\Gamma = 0$	36
5.1. Conceptual model of the source zone.	44

List of Figures (continued)

	Page
5.2. The area associated with the sampling point is shaded gray. The points above and below each sampling point are used to determine the height of the rectangle, and the point from the other well (to the right in this example) is used to determine the width of the block.....	46
5.3. Classical tritium transport for an instantaneous source. The solute travels downstream as a dispersing pulse.....	51
5.4. The mass discharge output file gives the mass discharge (D) across each plane at the x-intervals.....	53
5.5. Distribution of tritium tracer into zones 50 m long.	57
5.6. Plot of the tritium concentration distributions for the snapshot at 328 days at MADE-2. A box is drawn around the area defined as the source zone. The boundary separating the source from the plume zone is the downgradient side, the right side, of the box.....	59
5.7. Vertically averaged values of concentration (pCi/mL) measured at 27 days for the sampling wells located 15 – 20 m downgradient of the injection wells. The dashed lines highlight the range of concentrations near the centerline (y = 0 m) of the tritium distributions.	61
5.8. Mass distributions for the source - plume simulations in REMChlor for 3 different values of C_0 . The simulations are compared against the observed tritium distributions.....	66
5.9. Results for 27 days. The tritium distributions of the data (top) are compared with the REMChlor simulation (bottom). The crossed box in the simulation plot represents the source zone.....	68
5.10. Results for 132 days.....	68
5.11. Results for 224 days.....	69
5.12. Results for 328 days.....	69

List of Figures (continued)

	Page
5.13. Comparison of mass distribution plots calculated using REMChlor and using a dual-domain mass transfer (DDMT) model. The mass distributions calculated in REMChlor are labeled $C_0 = 40$ pCi/mL. The distributions calculated using a DDMT model are taken from Guan (2006).....	71
5.14. Concentrations along the centerline of the plume for the no-remediation case, and the source and plume remediation cases.....	75

CHAPTER 1 INTRODUCTION

Groundwater contamination is a problem at many sites where contaminants pose serious risks to people and to the environment that may be exposed to the contaminated groundwater. The groundwater remediation industry works to reduce the impact of these contaminants by monitoring and by site clean-up.

Transport of solutes in groundwater is controlled by many factors, such as the physical properties of the aquifer and the properties of the contaminant of concern. One class of tools used at sites with groundwater contamination are groundwater transport models. Models are used to simulate contaminant transport and to try to gain an understanding of how the contaminant distributions in the aquifer will evolve over time.

1.1 Solute Transport in Groundwater

Solutes dissolved in groundwater travel by advection and dispersion. Advection carries the solute with the groundwater velocity, and dispersion is caused by mixing and spreading. Dispersion is mainly due to the movement of solute around small-scale heterogeneities (Wang and Anderson, 1982). Solute transport can also be retarded by adsorption onto particles in the subsurface. In a uniform flow field advection only occurs in the downgradient direction, while dispersion will occur in three dimensions with little dispersion in the up-gradient direction. The governing equation for solute transport by advection and dispersion is referred to as the advection-dispersion equation. For a case

with a non-reactive solute, a uniform flow-field, and three-dimensional dispersion, the equation for the change in solute concentration (C) in time and space is

$$\frac{\partial C}{\partial t} = -v \frac{\partial C}{\partial x} + D_x \frac{\partial^2 C}{\partial x^2} + D_y \frac{\partial^2 C}{\partial y^2} + D_z \frac{\partial^2 C}{\partial z^2} \quad (1.1)$$

where v is the pore water velocity, and D is the dispersion term in the longitudinal (x), transverse (y), and vertical (z) directions. The advection-dispersion equation can be modified to account for various sources and sinks, such as mass decay or generation by chemical reactions. The equation can also be modified to consider retardation, where the solute moves slower than the advection rate would suggest, due to adsorption of the solute onto porous media surfaces (Wang and Anderson, 1982).

There are different ways of solving the governing equation for solute transport by advection and dispersion. Analytical solutions to the governing equation often require the user to make assumptions, such as a uniform flow field, to simplify the equation so that it can be solved. Numerical techniques can also be used to solve the governing equation. Numerical solutions require fewer simplifications, but they are also more computationally extensive and require more field data to determine the parameters.

Solute transport can be quite complex at sites that have a large degree of heterogeneity in the hydraulic conductivity field. The groundwater velocity is related to the hydraulic conductivity, so that groundwater will be able to flow faster through materials with a higher conductivity. It can be difficult or impossible to solve the advection-dispersion equation analytically for solute transport for a case where the velocity varies across the spatial extent of the site.

At heterogeneous sites preferential pathways can develop where the groundwater and solute flow more easily through material with a higher hydraulic conductivity. One variety of the advection-dispersion model for solute transport divides the model into two domains to simulate situations where there is a large degree of heterogeneity. This approach (the dual-domain method) assigns one zone a lower value of permeability and one a higher value. The two zones are coupled by a mass transfer term that describes the rate of solute transfer between the two zones. The dual domain models simulate transport as differential advection, where fluids move at different velocities in each zone (Guan et al., 2008). This acts to retard the solute at early times, where solute diffuses into the low permeability zone. At later times the solute in the low permeability domain diffuses back into the high permeability zone, acting as a source for the dissolved solute. Guan et al. (2008) describes a recent application of this approach to the MADE site.

1.2 Screening Level Models

Screening-level models are widely used at sites with groundwater contamination. Such models may not be as detailed as other more comprehensive models, but they require less time and resources to run. These models have several purposes, such as to determine the affected area, to compare the possible effects of different remediation approaches, and to assess risk.

There are a few of these screening-level models that are publicly available. McGuire et al. (2004) reviewed many sites that were contaminated with chlorinated solvents. This study found that at 60% of the sites computer models were used to

determine whether natural attenuation would be suitable. The most frequently used model was BIOCHLOR (McGuire et al., 2004).

BIOCHLOR is an analytical screening-level model intended for use at sites contaminated with chlorinated solvents. The model analyzes data for a site to find the length of the plume, the time it takes for the plume to reach its maximum length, and how long it takes for the plume to begin shrinking. Remediation by natural attenuation is considered by calculating the time it takes for the plume to stabilize and begin shrinking without the addition of any engineered features to increase remediation (Aziz et al., 2000).

The BIOCHLOR model is based on the Domenico (1987) solution for solute transport. BIOCHLOR has 1-dimensional advection and 3-dimensional dispersion. BIOCHLOR allows the user to specify retardation (by linear adsorption) and first-order reaction rates contributing to the decay of the parent compound and the formation of daughter products (Aziz et al., 2000; Aziz et al., 2002). BIOCHLOR also considers decay of the source zone. The source concentration can be constant or can be set to decay with time. BIOCHLOR uses a first-order source decay rate which can be set by the user (Aziz et al., 2002).

BIOSCREEN is another screening-level model for use at sites where natural attenuation is a viable remediation option. BIOSCREEN is intended for sites that have hydrocarbon contaminants from petroleum fuel spills (Newell et al., 1996). The BIOSCREEN model uses the 3-dimensional Domenico (1987) solute transport model, and considers 1-D advection, 3-D dispersion, adsorption, and first-order reactions

(Newell et al., 1996). Both BIOCHLOR and BIOSCREEN are available on the US EPA website.

The US EPA recently released a new screening-level model to its website (USEPA, 2008). This newer model, REMChlor, is designed for chlorinated solvents as is BIOCHLOR. One difference between REMChlor and BIOCHLOR is that REMChlor allows the user to consider various engineered remediation methods as well as natural attenuation (Falta, 2008). This modeling approach is described in more detail later in this thesis.

1.3 Tritium Tracer Experiments

Groundwater tracer experiments are performed at sites to gain information on the behavior of solutes in the subsurface. One type of experiment introduces a known amount of tracer to the aquifer, and the site is monitored over time. Observations of tracer distributions can provide information about the site such as the groundwater velocity, diffusion, dispersion, and retardation.

Tritium is sometimes used as a groundwater tracer at experimental sites because it is conservative and does not react with the aquifer materials. Because tritium is an isotope of hydrogen (^3H) it forms bonds with hydrogen and oxygen to create a water molecule, called tritiated water. Tritiated water is non-reactive and behaves like water in the subsurface (USEPA, 2007; USNRC, 2007). Because tritium is non-reactive, it would be expected to leave the source as a parcel of water and to travel downgradient of the injection site in accordance with the hydraulic conductivity distribution and the hydraulic

head gradients. In a homogeneous aquifer, an injected tritium tracer would be expected to move downgradient as a pulse with 3-D dispersion.

1.4 Objectives

The main objective of this study was to determine if a simple screening-level model can capture the main features of a tritium plume in a heterogeneous aquifer. This study tests to see if a model designed for sites with NAPL (nonaqueous-phase liquid) contamination can be applied to the MADE-2 data for tritium, which resembles the plumes that evolve at sites with NAPLs. In this study the REMChlor model is used to simulate the tritium distributions seen at the MADE-2 site.

Initially tritium transport is simulated to produce the classical case where tritium is introduced to the aquifer instantaneously and is not retarded during transport. The subsequent simulations focus on modeling the tritium distributions seen at MADE-2. These simulations use a concept designed to represent NAPL-contaminated sites, and consider the region near the injection site as a source zone and the downstream area as the plume zone. The source and plume are modeled differently, but are coupled together so that the source output is equivalent to the plume input.

The simulations were calibrated by considering the parameters used to define the source zone and the parameters that control transport in the plume region. The simulations were matched to the observed mass distributions of tritium for the length and width of the plume.

CHAPTER 2

MADE SITE ANALYSIS

The MAcroDispersion Experiments (MADE) were performed to study transport in a highly heterogeneous alluvial aquifer. There have been two MADE experiments conducted at the Columbus Air Force Base in Mississippi. The MADE-2 experiment involved the injection of tritium and four other compounds, which were then measured at locations downgradient to characterize tracer migration (Boggs et al., 1993).

2.1 Site Characterization

As described in Boggs et al. (1990), the MADE site is located in Lowndes County in northeastern Mississippi. The site is approximately 0.25 square kilometers and is situated just south of the Buttahatchee River and about 6 km east of the Tombigbee River. The site slopes gently to the north, with an elevation difference of approximately 1 m between the southeastern corner and the northern boundary of the site Figure 2.1.

2.1.1 Geologic Description

The aquifer is composed of Pliocene aged alluvial terrace deposits associated with the Buttahatchee River and has an average thickness of approximately 11 meters. The aquifer can be divided into two layers—the top layer being comprised of meandering fluvial sediments, and the lower aquifer layer was formed by braided fluvial deposits

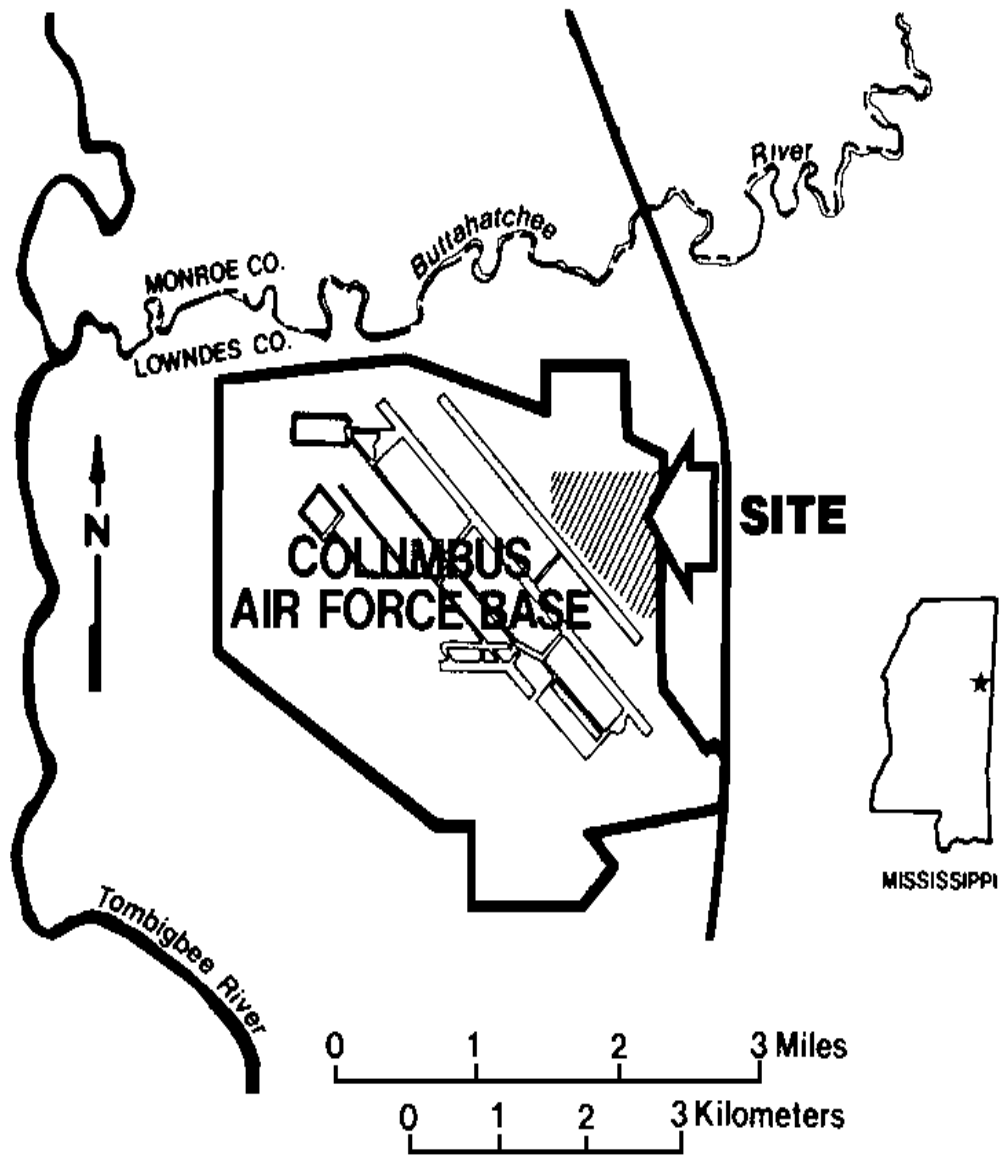


Figure 2.1 MADE site location. (Boggs et al., 1990)

(Bowling et al., 2006). The sediments of the aquifer range from well to poorly-sorted sands and gravelly sands with some silt and clay (Boggs et al., 1992).

Cretaceous aged clay material of the Eutaw Formation creates an aquitard and represents the lower boundary of the aquifer. There are two layers to the Eutaw Formation, with fine sands and silts dominating the upper part of the formation and clays dominating in the lower part (Boggs et al., 1990; Bowling et al., 2006).

Measurements of average bulk density and porosity were taken from 84 soil cores (Boggs et al., 1992). The average bulk density for aquifer materials is 1.77 g/cm^3 . The average porosity is 0.31 with a standard deviation of 0.08. Compaction of the soil samples may have occurred during sampling, so a porosity value of 0.35 may be a better approximation (Boggs et al., 1992).

2.1.2 Hydrologic Setting

The MADE site receives an annual average of 144 cm of rain. The rainfall is fairly evenly distributed across the year, with the wettest months in the winter and early spring. Approximately 40% of total rainfall contributes to the net recharge to the aquifer from infiltration (Boggs et al., 1990). The aquifer at the MADE site is unconfined, so the water levels in the aquifer respond to variable rates of infiltration. Seasonal influences on the water table range from 2 to 3 m (Boggs et al., 1992). The water table elevations were measured at two different elevations in one well. The deep measurement was at 56.3 m above sea level, and the shallow measurement was at 61.1 m (Boggs et al., 1990). Figure 2.2 shows the variations in the water table between June 1990 and September 1991 (the MADE-2 experiment began in June 1990).

The infiltration rate causes the saturated thickness of the aquifer to vary by 20 – 30% annually (Boggs et al., 1990; Boggs et al., 1992). The average hydraulic gradient at the site is approximately 0.003, and it fluctuates seasonally between 0.002 and 0.005 (Boggs et al., 1992). The seasonal changes in gradient seem to have little to no influence on the groundwater flow direction. The gradient direction was northward throughout the experiment (Boggs et al., 1992).

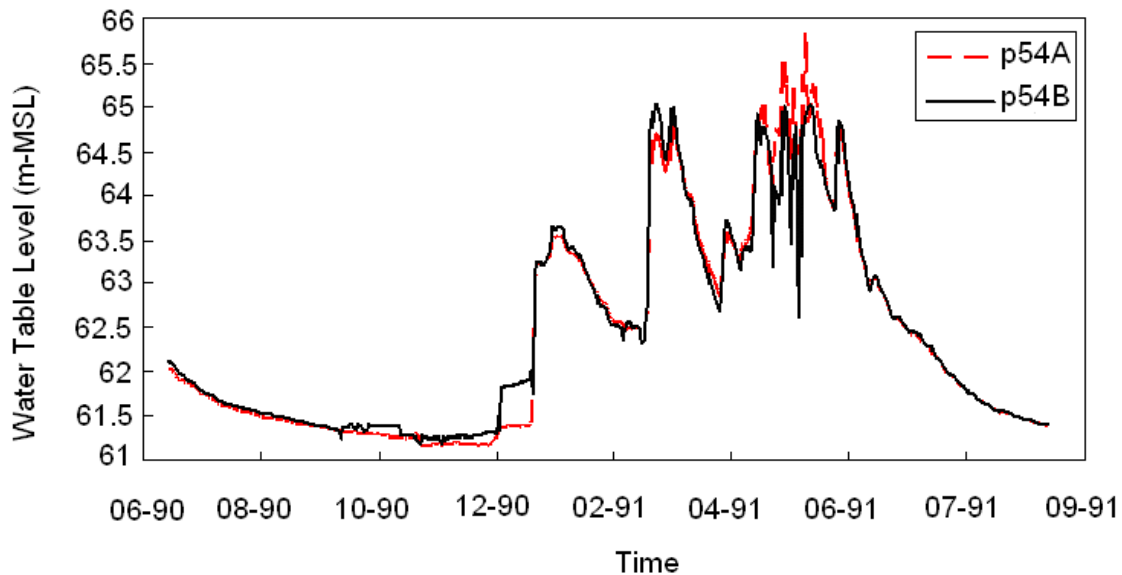


Figure 2.2 Variations in water table elevation between June 1990 and September 1991 in well p54 at 2 depths: shallow (p54a) and deep (p54b). (Guan, 2006).

Hydraulic conductivity measurements were taken across the site using several methods. The largest number of conductivity measurements came from borehole flowmeter tests. There were 2187 measurements taken at varying depths in 49 wells (Boggs et al., 1993). Two large scale pump tests were conducted centered at two different sites. The first pump test was located 80 m southeast (upgradient) of the

injection wells, and the second was located 60 m north (downgradient) of the injection site (Boggs et al., 1992). The other methods used for collecting conductivity data were slug tests, and permeameter tests on collected soil cores were performed in the laboratory. The borehole flowmeter measurements show similar results to the large scale pump tests and cover the site in greater detail (Boggs et al., 1992; Rehfeldt et al., 1992; Boggs et al., 1993). The flowmeter measurements were chosen as the primary source for conductivity data because they were consistent with the large-scale tests and are more cost effective. The flowmeter measurements cost 3 times less than the permeameter tests and 41 times less than the slug tests (Rehfeldt et al., 1992).

Results from the conductivity measurements illustrate the heterogeneity of the aquifer. Figure 2.3 shows the vertical conductivity profile down the longitudinal axis of the site. The conductivities measured in each test well vary by up to four orders of magnitude along the depth of the well. The area near the injection site (the near-field) has a conductivity of approximately 10^{-3} cm/s, while conductivities increase one to two orders of magnitude 20 m downgradient (Boggs et al., 1992; Rehfeldt et al., 1992; Boggs et al., 1993).

The conductivities vary with elevation between the near-field and far-field. In the near-field the conductivity is higher below an elevation of 58 m MSL. In the far-field 20 to 30 m downgradient of the injection site the conductivity is higher above an elevation of 58 m. The sediments in the aquifer are made up of deposits from a braided stream overlain by deposits from a meandering stream. The boundary between these two sedimentary environments occurs at approximately 58 m, which corresponds with the

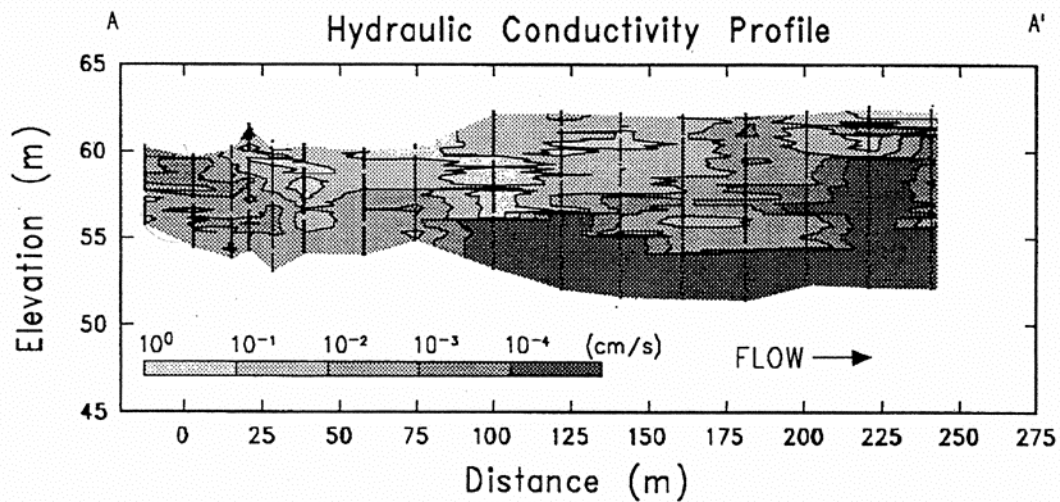


Figure 2.3. Hydraulic conductivity along the centerline. (Boggs et al., 1993)

variability in the hydraulic conductivity (Rehfeldt et al., 1992). The deposits left by the braided stream have a higher value of conductivity than the meandering stream deposits, and the majority of the data collected at the site are taken from the portion of the aquifer composed of braided stream deposits (Guan, 2006).

The central region of the longitudinal profile (between 20 and 160 m downgradient of the injection site) has higher values of conductivity (Figure 2.4). This corresponds to a channel of the meandering stream. The meander is situated at a 45 degree angle to the direction of groundwater flow. The flow does not seem to go along the axis of the channel. Rehfeldt et al (1992) treat the meander simply as a region of high conductivity.

The hydraulic head was mapped at the site, from which contour plots of the potentiometric surface were created (Figure 2.5). The potentiometric surface reflects the distribution of hydraulic conductivities. In the far field where the conductivity is highest,

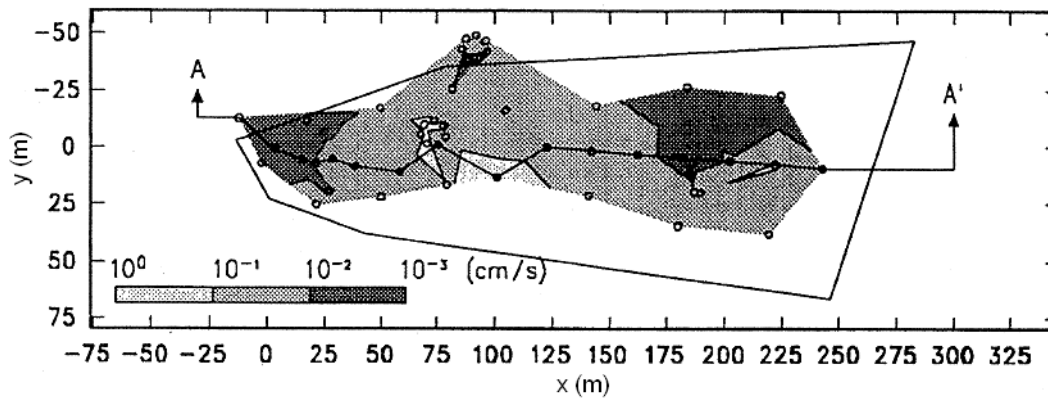


Figure 2.4. Depth-averaged hydraulic conductivity profile. (Boggs et al., 1993)

contour lines are widely spaced, representing a smaller hydraulic gradient. The near field shows a larger hydraulic gradient, due to the lower conductivities in the region.

The potentiometric surface shows an interesting feature in the near field where the contours form a V-shaped pattern. This pattern indicates an area where groundwater flow converges towards a zone of higher conductivity and increasing groundwater velocity. This zone and the far field have a groundwater velocity of about 159 m/yr, while the near field has an approximate velocity of 5-10 m/yr (Boggs et al., 1990). The converging zone represents a preferential flow path for water moving downgradient from the injection location.

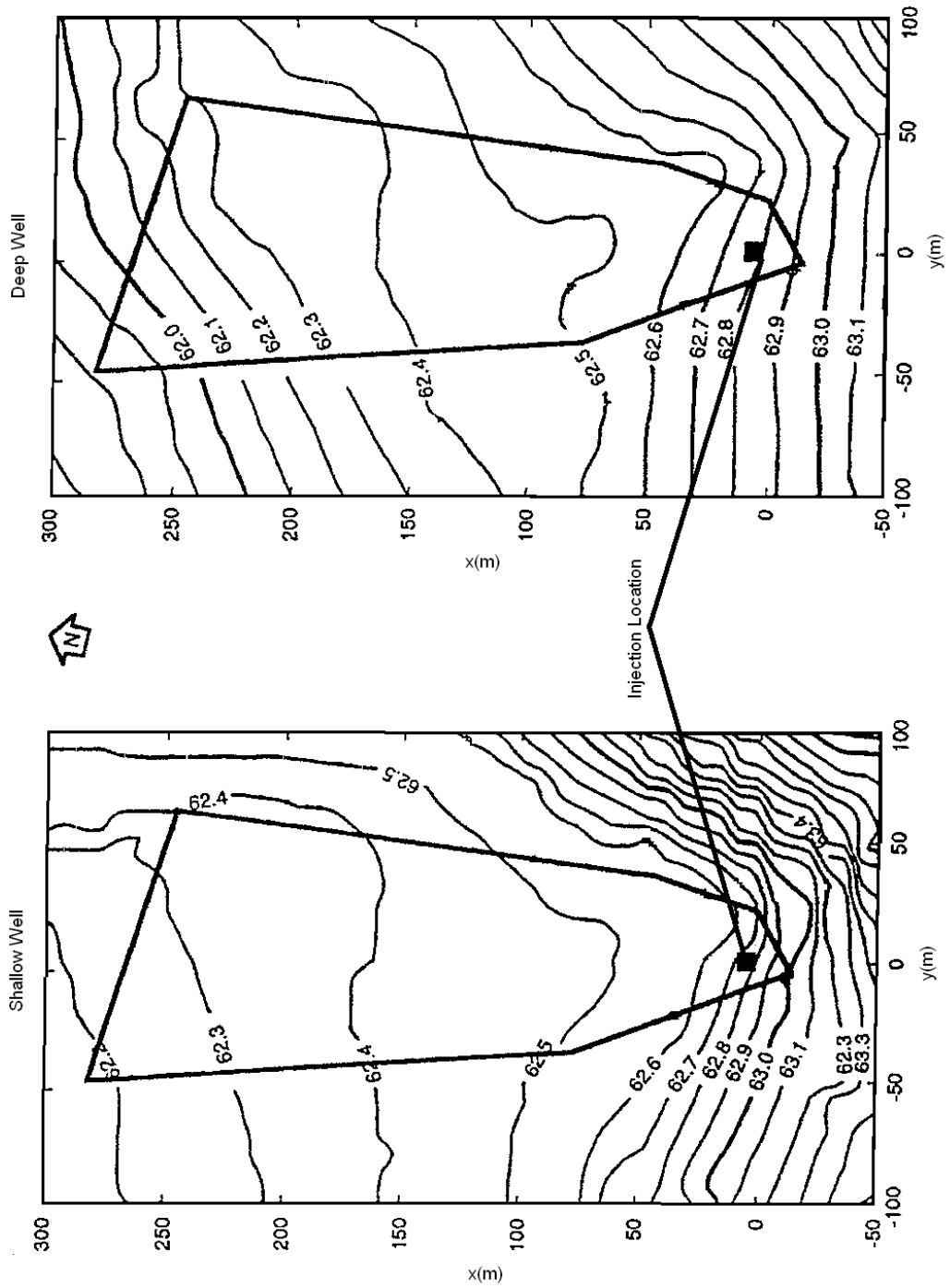


Figure 2.5. Maps of the potentiometric surface for June 1990 head measurements. (Boggs et al., 1993).

2.2 Tracer Experiment

The MADE site has been the location of three large-scale tracer experiments. There have been two MADE experiments, the second one being the focus of this study, and one natural attenuation study (NATS). The main goal of these studies was to develop a dense monitoring network to compare fluid-flow and transport models against collected data (Bowling et al., 2006).

2.2.1 Tritium Tracer Experiment Setup

The MADE-2 experiment studied the transport of tritium and four organic compounds under natural gradient conditions. Boggs et al. (1993) describes the methods and results of the tracer tests. The tracer was injected into five wells spaced 1 m apart in a linear array. Each injection well was screened over 0.6 m, between the elevations of 57.5 and 58.1 m. The injection solution consisted of the tracers mixed with water from a well upgradient of the injection location to a total volume of 9.7 m³. The amount of tritium mixed in the total solution was 0.5387 Ci, giving the solution of tritium a concentration of 55,610 pCi/mL.

Tritium Tracer Test Parameters	
Total Activity	0.5387 Ci
Concentration	55,610 pCi/mL
Injected Volume	9.7 m ³
Injection Period	2 days
Sampling Times	27, 132, 224 & 328 days

Table 2.1. MADE-2 tracer test parameters

Tracer transport was monitored using the 328 multilevel samplers (MLS) installed at the site. The MLS captured samples at 20 to 30 different depths, creating a three-dimensional image of tracer concentrations. Figure 2.6 shows the distribution of the sampling wells. The experiment was conducted over 15 months, beginning June 26, 1990. Five sampling events, or snapshots, were conducted about 100 days apart. The fifth snapshot at 440 days did not capture the leading edge of the tritium plume and was not used to analyze the tritium transport at MADE-2 (Boggs et al., 1993).

2.2.2 Tritium Distribution

The tritium data collected during the four different sampling snapshots were used to study the tracer behavior. The tritium concentrations were collected at sampling points over the study area, and these concentrations were interpolated to create a map of the tracer distributions. The data were interpolated for this study using the inverse-distance weighting method with an exponent of four. The interpolation and maps were done using Tecplot software (Amtec Engineering, 2003). The concentrations were normalized to the tritium concentration of the injection solution to help compare the results for each snapshot.

Figure 2.7 shows the tritium tracer plumes at an elevation of 59 m for the four sampling snapshots. The plots illustrate asymmetry of the plume in the longitudinal (x) direction. The final snapshot of the tritium plume at 328 days shows that the highest concentrations stay within 20 m of the injection point. The leading edge of the plume, however, extends over 260 m downgradient and has concentrations two orders of magnitude lower than those near the injection location.

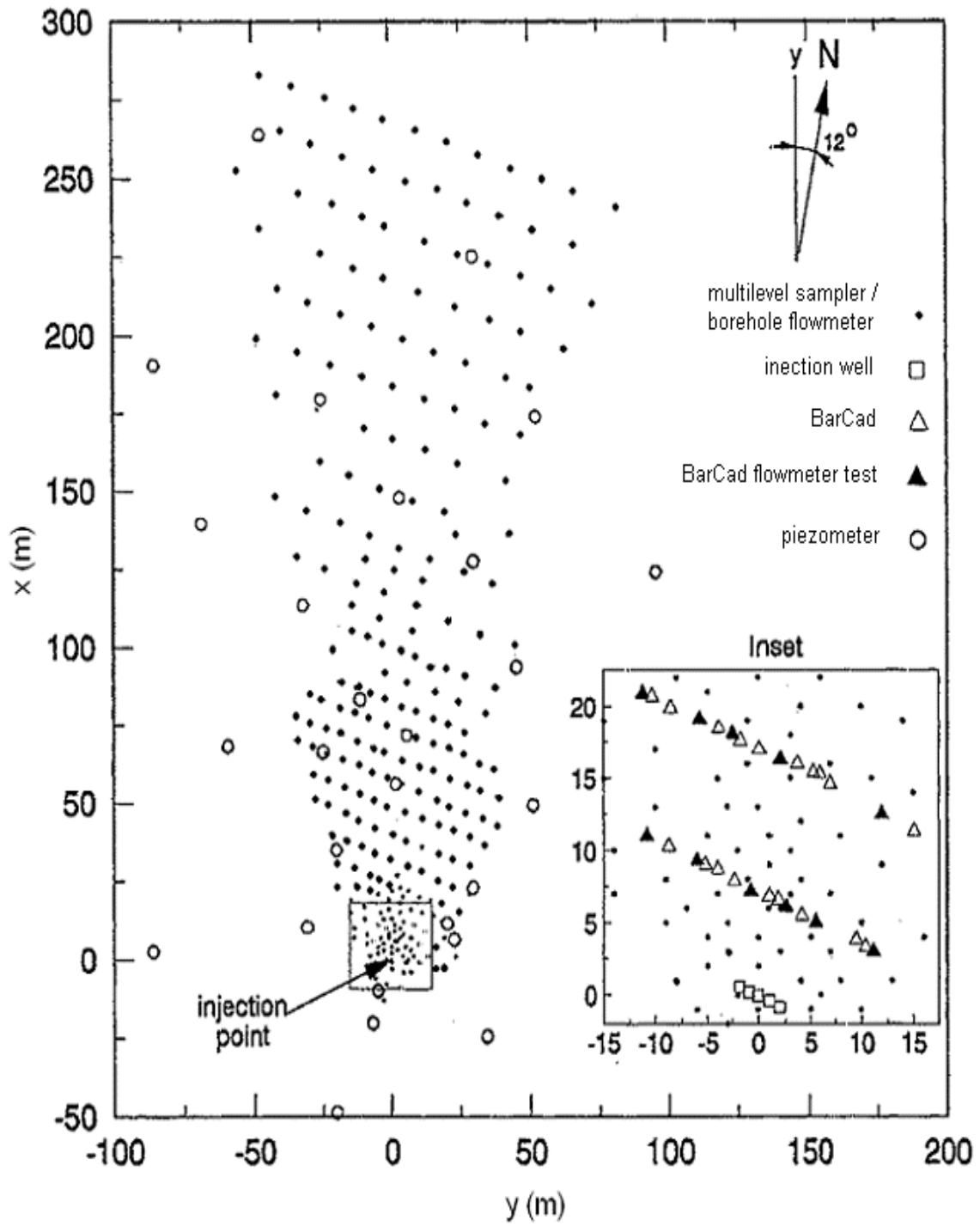


Figure 2.6. Sampling network. (Boggs et al., 1993).

Figure 2.8 shows vertical slices of the tritium plumes along the centerline, $y = 0$. The vertical slices show the extreme vertical heterogeneity. The plot for the final snapshot at 328 days shows a dashed line representing the elevation used to generate the horizontal plots. This elevation approximately divides the low conductivities in the near-field (below 59 m) from the higher conductivities in the far-field, where the majority of the leading edge of the plume lies above 59 m.

The concentrations are consistent with the variable conductivity distributions, as discussed above. Figure 2.9 compares the vertical conductivity distribution alongside the vertical slice for the final snapshot. The region that includes the injection location and the area extending 20 m downgradient has a low conductivity at 10^{-3} cm/s. In the far-field the conductivity increases by one to two orders of magnitude, and the highest values of conductivity are above an elevation of 59 m. The tritium distribution at 328 days shows that in the far-field the majority of the tracer lies about the line drawn at an elevation of 59 m.

The groundwater velocity varies in the same manner as the hydraulic conductivity. The near-field velocity has an average of 5 m/yr, while the far-field velocity increases to an average of 400 m/yr (Boggs et al., 1993). These differences in groundwater velocity along the longitudinal axis of the plume contribute to the extreme asymmetry in the longitudinal direction. The injected tracer in the near-field ($x < 20$ m) is slow to leave the injection zone but speeds up by a few orders of magnitude once it reaches a region of higher conductivity. The low concentration leading edge of the plume continues to travel downgradient at a much faster rate than that of the tracer

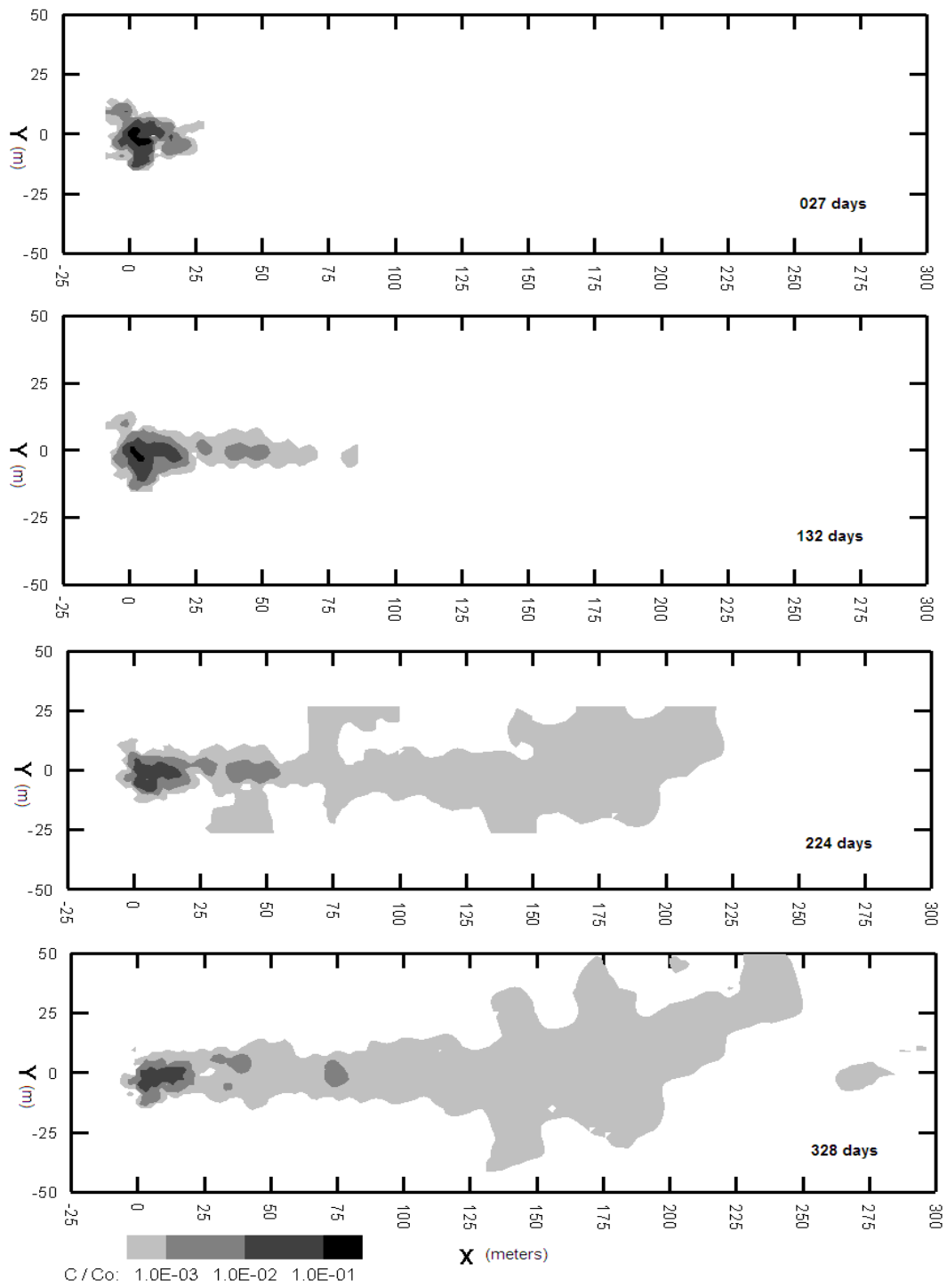


Figure 2.7. Tritium concentrations at an elevation of 59 m for the 4 snapshots.

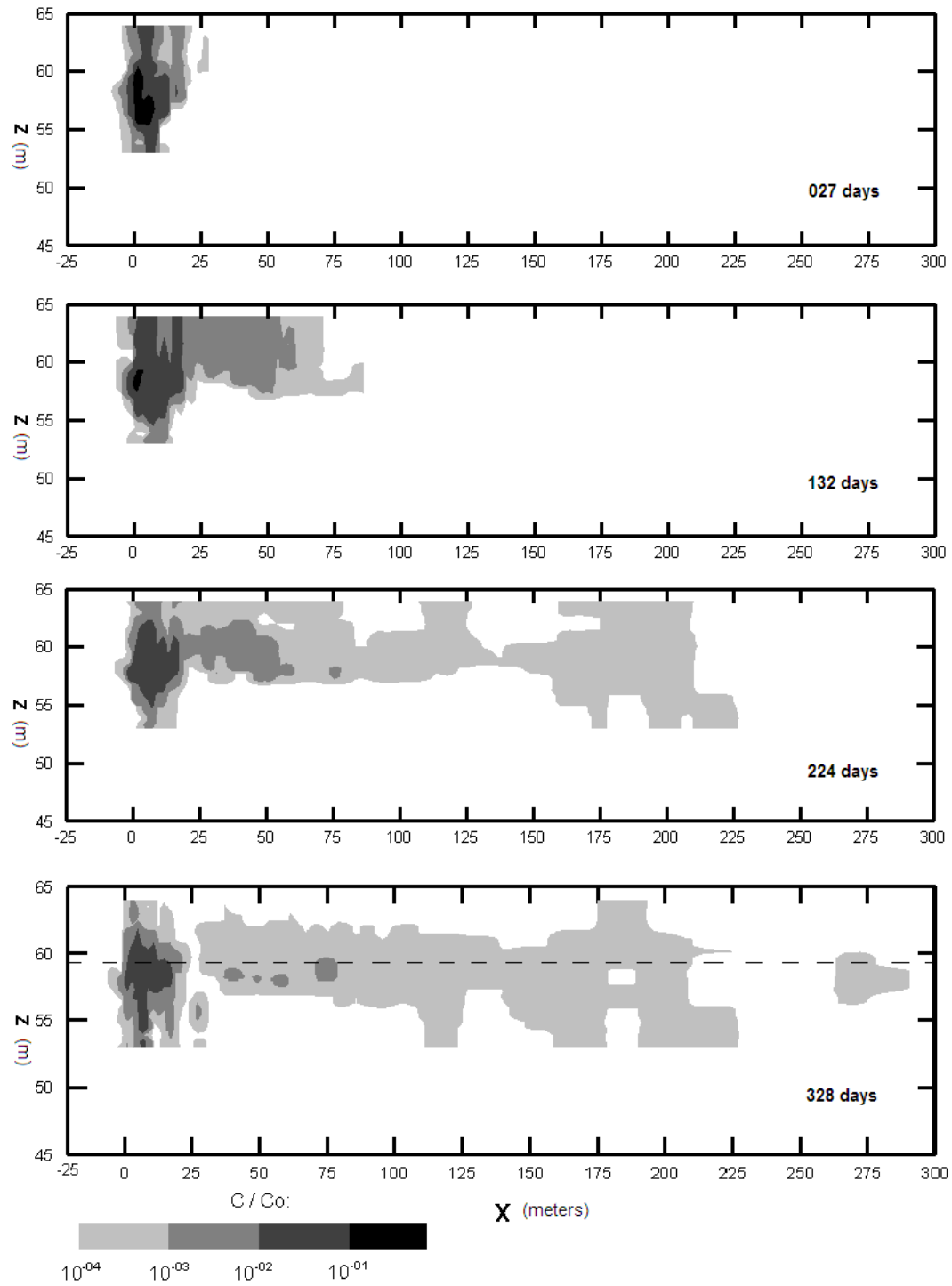


Figure 2.8. Tritium distributions along the centerline of the plume.

leaving the near-field region.

The variability in hydraulic conductivity also contributes to the longitudinal asymmetry of the tracer plume. The tracer coincides with the areas with high hydraulic conductivity, which suggests that the tracer flows along preferential flow paths. The preferential flow paths would exist due to the variability in conductivity. Mass transfer between the zones of high permeability, such a preferential flow paths, and low conductivity is also likely to play a large role in the non-uniform tracer transport.

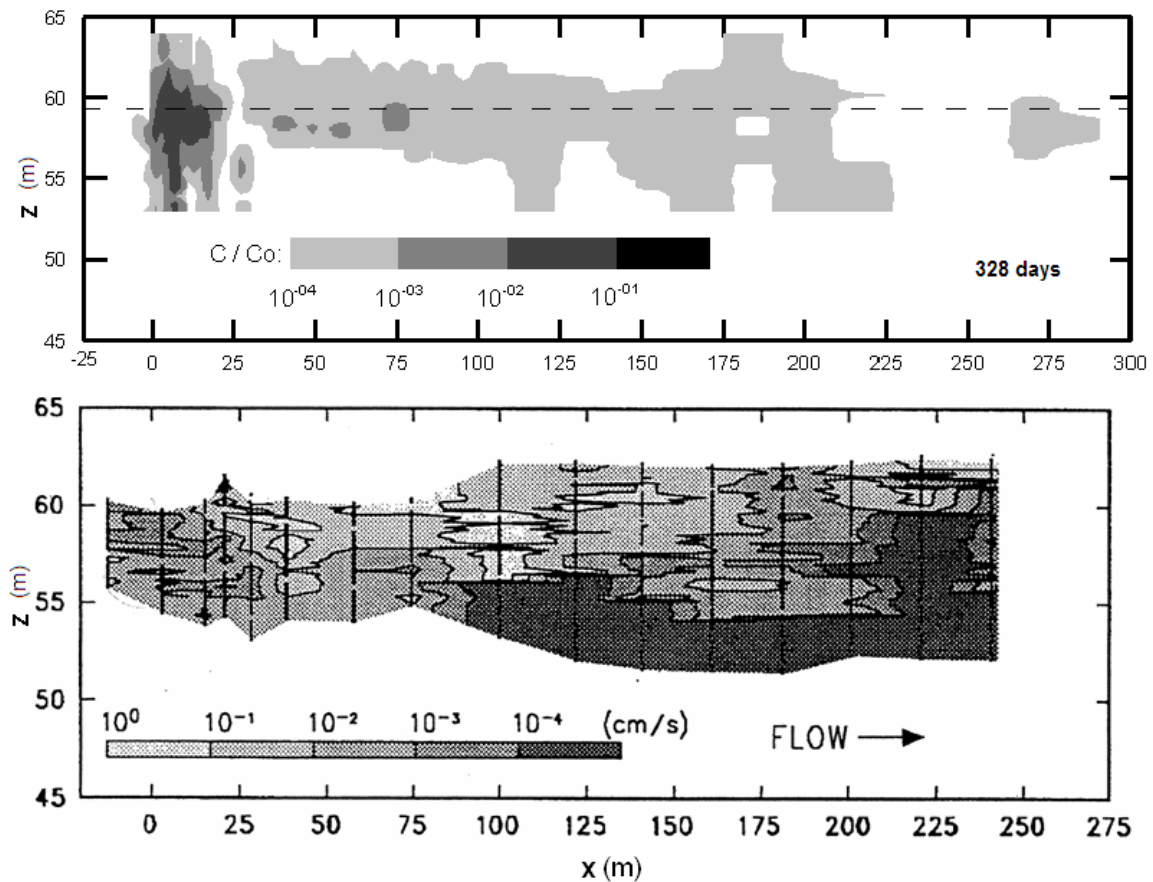


Figure 2.9. Tritium distribution at 328 days (top) compared with hydraulic conductivity distribution (bottom, modified from Boggs et al., 1993) along the centerline of the site.

CHAPTER 3 PREVIOUS STUDIES

The purpose of the MADE experiments was to measure a dense data set of aquifer properties and contaminant transport in a heterogeneous aquifer to test models and theories about the relationship between hydraulic conductivity and transport (Harvey and Gorelick, 2000; Bowling et al., 2006). These experiments have been studied extensively using a variety of approaches (Eggleston and Rojstaczer, 1998; Zheng and Jiao, 1998; Feehley et al., 2000; Harvey and Gorelick, 2000; Zheng and Gorelick, 2003; Bowling et al., 2006; Guan, 2006; Guan et al., 2008). Several modeling schemes have been applied to MADE to describe the non-classical transport seen at the site.

3.1 Spatial Moments Analysis

A spatial moment analysis of the tritium concentration data is included in Boggs et al. (1993) to calculate the tritium mass (zeroth moment) and center of mass (first moment) during the experiment. The analysis provides quantitative results for comparison of each snapshot of the plume. The estimates of mass are used to test the sampling validity by comparison of the known injected mass with those calculated.

The mass in the plume is found from the zeroth moment associated with the concentration data

$$M_T = \iiint \theta C dx dy dz \quad (3.1)$$

where C is the tracer concentration and θ porosity. The porosity is assumed to constant in this analysis (Boggs et al., 1993).

The plume's center of mass (x_c, y_c, z_c) is found by the first moment

$$x_c = \frac{\iiint \theta C x dx dy dz}{M_T}, \quad y_c = \frac{\iiint \theta C y dx dy dz}{M_T}, \quad z_c = \frac{\iiint \theta C z dx dy dz}{M_T} \quad (3.2)$$

The value of porosity does not affect the center of mass calculations as it can be cancelled out from the porosity term used to find M_T Equation (3.1) (Boggs et al., 1993).

The zeroth and first moments for the tritium plume were calculated for each snapshot. The calculated mass in the plume varied between the four snapshots. The analysis overestimates mass at early times and underestimates mass at later times. The range of values for mass calculated by the spatial moment analyses range from 152% at 27 days to 77% at 328 days. The estimated values of total mass normalized to the injected mass (M/M_0) and center of mass (X_C) are given in Table 3.1 (Boggs et al., 1993).

Time [days]	M/M₀	X_c [m]
27	1.52	3.9
132	1.05	8.1
224	0.98	46.5
328	0.77	76.8

Table 3.1. Results of the spatial moment analysis at each snapshot (Boggs et al., 1993).

Adams and Gelhar (1992) and Boggs et al. (1993) offer several explanations for the discrepancies between the calculated mass and the actual injected mass. The

overestimation at early times is probably due to preferential sampling from high permeability zones. The injected tracer will initially appear in zones of high hydraulic conductivity, and diffuse into zones with lower conductivity as time increases. The MLS will capture the tracer in the high conductivity zones much more easily than the tracer that is trapped in low permeability material. The sampled mass is averaged over the entire domain, which includes both the zones with high and low permeability. At early times the impermeable zones will contain relatively clean water, and the majority of the tracer mass will be in the permeable zone. Samples collected at this time will draw mass from the permeable zone, and that mass will be averaged over the entire area. At later times some of the mass will have diffused into the low permeability zones, which are not sampled from very well. This accounts for the overestimation at the beginning of the experiment, and contributes to the underestimation of mass at later time periods (Adams and Gelhar, 1992; Boggs et al., 1993). This phenomenon is better described in a later study by Guan et al. (2008).

Under estimation at the end of the experiment is also due to plume truncation. The data taken at 440 days could not be used for the tritium tracer because it failed to capture the leading edge of the plume. The measurements taken at 328 days were more complete but there was still some minor truncation that could result in mass underestimation (Boggs et al., 1993).

The average velocities of the center of mass for each sampling period are found by calculations of the first moment of the tritium plume. The average longitudinal

velocity is equivalent to the distance traveled by the center of mass in the x-direction for each time period

$$v_i = \frac{x_i - x_{i-1}}{t_i - t_{i-1}} \quad (3.3)$$

The center of mass at $t = 0$ days is assumed to be 0 m.

An analysis of the mean velocity was conducted in Guan (2006). Table 3.2 shows the calculated values of velocity for the time period leading up to the snapshot. Figure 3.1 shows the longitudinal displacement as a function of time. The steepness of the slope for each sampling period indicates the mean velocity during that time period. Prior to 132 days where the slope in Figure 3.1 is fairly gradual, the mean tracer velocity is 0.04 m/d. After 132 days the mean velocity increases 10-fold to 0.42 m/d. This represents where a substantial amount of the tracer makes its way to the higher conductivity zone about 20 m downgradient of the injection point (Guan, 2006).

Time [days]	V [m/d]
27	0.14
132	0.04
224	0.42
328	0.29

Table 3.2. Velocity values for the time period leading up to each snapshot. Calculated from center of mass estimates.

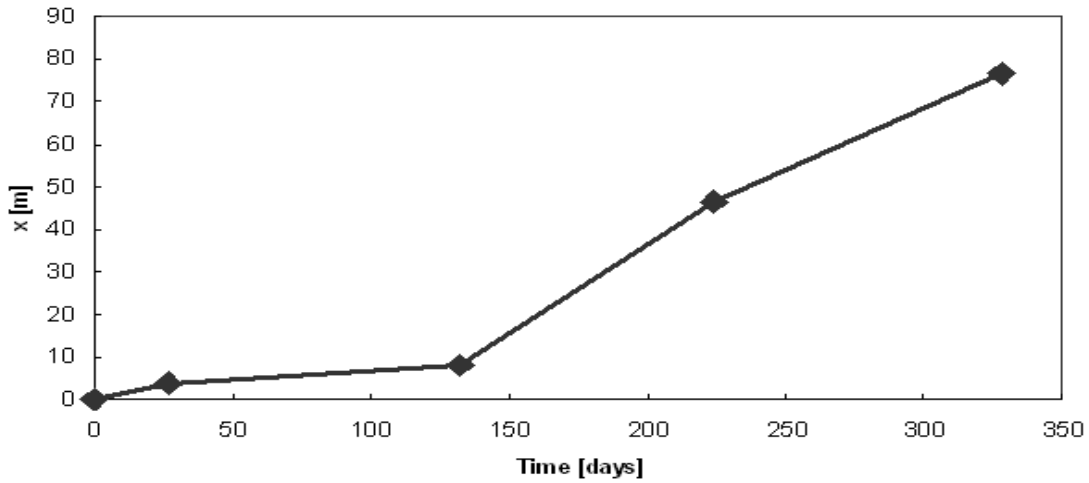


Figure 3.1. Longitudinal center of mass displacement for 4 snapshots. (Data from Boggs et al 1993).

3.2 Single-Domain Advection-Dispersion Models

Most models consider advection and dispersion as the primary mechanisms for transport in the aquifer. These models are based on the advection-dispersion equation (ADE), where the transport processes (advection, dispersion, adsorption, reactions, etc.) are related to the conservation of mass. The most basic form of the advection dispersion equation is

$$\frac{\partial C}{\partial t} = -v \frac{\partial C}{\partial x} + \alpha_x v \frac{\partial^2 C}{\partial x^2} \quad (3.4)$$

for a 1-dimensional case with no retardation or reactions. The first term on the right hand side describes advection due to the pore-water velocity (v), and the second term concerns dispersion in the x -direction where α_x is the longitudinal dispersivity. This can be expanded into 2 or 3 dimensions for dispersion by including transverse and vertical

dispersion terms, $\alpha_y v \frac{\partial^2 C}{\partial y^2}$ and $\alpha_z v \frac{\partial^2 C}{\partial z^2}$ respectively. The ADE can be modified to include retardation and reaction rates. For a uniform flow field, the ADE with 3-D dispersion, retardation and reaction rates is

$$R \frac{\partial C}{\partial t} = -v \frac{\partial C}{\partial x} + \alpha_x v \frac{\partial^2 C}{\partial x^2} + \alpha_y v \frac{\partial^2 C}{\partial y^2} + \alpha_z v \frac{\partial^2 C}{\partial z^2} + rxn(x, t) \quad (3.5)$$

Several studies applied the ADE model to MADE-2 (Eggleston and Rojstaczer, 1998; Zheng and Jiao, 1998; Feehley et al., 2000; Harvey and Gorelick, 2000). The ADE models were built around the hydraulic conductivity (K) distribution, which had to be interpolated from the data to fit the grid-scale of the models. Due to the heterogeneity in conductivity at the site, the data for the K-field may miss a lot of detail that exists at a smaller scale than that of the sampling network. Zheng and Jiao (1998), Feehley et al. (2000), and Bowling et al. (2006) compared different interpolation schemes for determining the K-field. They found that the model is sensitive to how the K-field is interpolated.

The results of these single-domain ADE models do not adequately describe the tritium distributions seen at the site. The ADE models do show the peak mass within 20 m of the injection wells, but they fail to capture the low concentration leading edge. The inability of the ADE models to describe transport at low concentrations is most likely due to the difficulty in representing the hydraulic conductivity field at the sub-gridblock level. The K-field varies over a much smaller scale than is practical to build into a model. The small-scale variations in the K-field lead to preferential flow paths and mass transfer

between zones with high and low conductivities (Zheng and Jiao, 1998; Feehley et al., 2000; Harvey and Gorelick, 2000).

3.3 Dual-Domain Mass Transfer Models

Several studies at the MADE site use dual-domain mass transfer (DDMT) models to describe the observed transport (Feehley et al., 2000; Harvey and Gorelick, 2000; Flach et al., 2004; Guan, 2006). DDMT models divide the aquifer into two domains, a high permeability mobile zone and a low permeability immobile zone. Mass transfer occurs between the two zones (Figure 2.1). The portion of the tracer in the mobile domain is transported by advection-dispersion, while tracer in the immobile zone is relatively stationary. The mass transfer between the two domains is driven by diffusion due to concentration differences or slow advection.

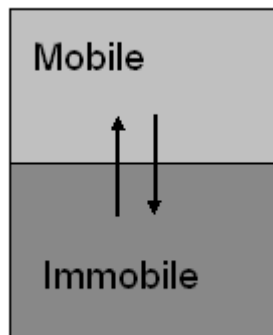


Figure 3.2. Concept behind DDMT models. The aquifer is divided into a mobile and immobile domain with mass transfer between each zone.

Harvey and Gorelick (2000) state that for a model of the MADE site to represent the physical processes the model must account for the fact that the observed mass changes over time. DDMT models can account for this because of the mass transfer between the two zones. At early times the majority of the tracer will be in the mobile domain, while the immobile domain will contain clean water. The samplers will preferentially extract water from the mobile region and average that concentration over both domains, causing the overestimation of mass. Later in time tracer will diffuse into the immobile domain and clean water may move into the immobile domain, causing the mass to be undersampled in the high conductivity zones.

DDMT models produce differential advection spreading, where the mobile portion of the tracer is moved downstream at early times while the immobile portion remains stationary. At later times, tracer in the immobile region upgradient of the initial parcel diffuses into the mobile domain and is advected downstream, resulting in long-term tailing (Flach et al., 2004).

DDMT models are valid at sites where mass transfer between the two domains occurs on the same time scale as the experiment. At the MADE site the time scale for solute diffusion between the two domains ranges between approximately 62 and 248 days (Harvey and Gorelick, 2000). This matches the period over which the MADE-2 experiment was observed, between 27 to 328 days. This indicates that mass transfer is significant for the period of the MADE-2 experiment.

Feehley et al. (2000) compared results from DDMT and single domain ADE models using two different interpolation schemes for interpreting the hydraulic

conductivity. They found that the DDMT approach matched the observed data for MADE-2 better than the ADE models regardless of which K-field was used. The dual-domain approach allows for anomalous transport mechanisms that occur at a smaller scale than the model grid. This incorporates transport that occurs along centimeter to decimeter scale conductivity heterogeneities and preferential flow paths (Zheng and Gorelick, 2003). Their results also indicate that the apparent mass transfer rate may vary in time or distance from the injection site if a first order approach is used.

There is evidence at the MADE site to support the existence of preferential flow paths. Outcrops near the MADE site show permeable structures on the centimeter to decimeter scale in contact with low permeability units (Zheng and Gorelick, 2003).

Typically, DDMT models use a constant rate for mass transfer across the experiment. Guan (2006) considered whether the first order mass transfer rate at the MADE site is scale dependent and changes with the duration of the experiment. This study shows that a scale-dependent mass transfer rate that decreases in time captures the observed distributions better than a constant value for mass transfer. The apparent mass transfer rate decreases with the experiment duration. The study also points out that the low hydraulic conductivity and some other, currently unexplained, trapping mechanism near the injection site might contribute to the initial slow advection, rather than mass transfer being the only process controlling the transport (Guan, 2006; Guan et al., 2008).

CHAPTER 4 REMCHLOR

REMChlor is an analytical model which couples source and plume behavior, designed for use at sites with non-aqueous phase liquid (NAPL) contamination. It considers the effects of different remediation types on both the source and the plume. The EPA has developed a graphical user interface for REMChlor which simplifies the processes of entering input values and reviewing the results.

REMChlor is designed to be a screening-level model and is much simpler than the models mentioned in Chapter 3. The tritium tracer test during the MADE-2 experiment has been extensively studied using these comprehensive models. Use of REMChlor to describe tritium transport at the MADE site offers a simpler alternative to the complex models previously used at the site.

4.1 Mathematical Model

The mathematical model is described in Falta (2008). In REMChlor a contaminated area is divided into two zones: the source and the plume (Figure 4.1). A mass balance on the source zone is solved for analytically and allows for source depletion by considering dissolution of the source mass, first-order decay, and remediation by delayed removal of the source mass. The plume model considers 1-D advection, 3-D dispersion, and retardation of the contaminant leaving the source zone, with parent-daughter decay reactions that can be a function of space and time.

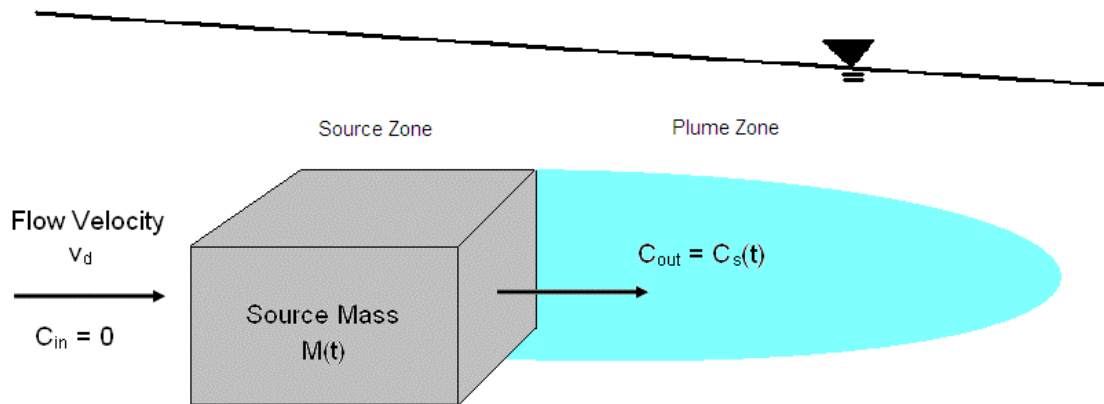


Figure 4.1. Conceptual model of coupled source and plume zones. (Modified from Falta et al., 2007.)

4.1.1 Source Model

The source zone is typically defined as the location where a contaminant enters the subsurface and the immediate surroundings. This region is characterized by very high contaminant concentrations. It can be difficult to directly measure the mass of contaminant in the source zone. The change in the source mass (M) depends on the rate of dissolution and flushing, and the rate of decay by mechanisms other than dissolution.

The mass balance on the source zone is given by:

$$\frac{dM}{dt} = -Q(t)C_s(t) - \lambda_s M \quad (4.1)$$

Mass loss due to dissolution is represented in the first term on the right hand side, where $Q(t)$ is the volumetric rate that uncontaminated water flows through the source zone and $C_s(t)$ is the time-dependent discharge concentration leaving the source. The second term

on the right side accounts for decay by other processes, where λ_s is the decay rate. In this study where tritium is the solute of concern, this term refers to radioactive decay.

Several experiments have shown a relationship between source mass and the discharge concentration leaving the source zone. This relationship can be approximated by a simple power function (Falta et al., 2005):

$$\frac{C_s(t)}{C_0} = \left(\frac{M(t)}{M_0} \right)^\Gamma \quad (4.2)$$

The value of Γ determines the shape of the curve—the response of the source discharge as the mass in the source changes (Figure 4.2). When $\Gamma = 1$ the source mass and discharge concentration have a 1:1 relationship. Values of Γ greater than 1 have a curve that lies below the 1:1 line, while values less than one produce curves that fall above the line. The simplest case occurs when $\Gamma = 0$, where the source mass decreases at a constant rate. This yields the scenario where the discharge concentration is constant until the source is completely depleted. Experimental data suggest that a Γ value of one is a reasonable approximation for many sites, though there can be some variability depending on the relationship between contaminant distribution and permeability (Falta et al., 2005).

The power function (4.2) can be combined with the source mass balance (4.1) assuming constant water flow rate, Q , through the source zone. This substitution gives

$$\frac{dM}{dt} = -\frac{QC_0}{M_0^\Gamma} M^\Gamma - \lambda_s M \quad (4.3)$$

The equation is nonlinear except for Γ values of zero and one. Falta et al. (2005) solved the equation using Bernoulli's transformation. These solutions are used in REMChlor to

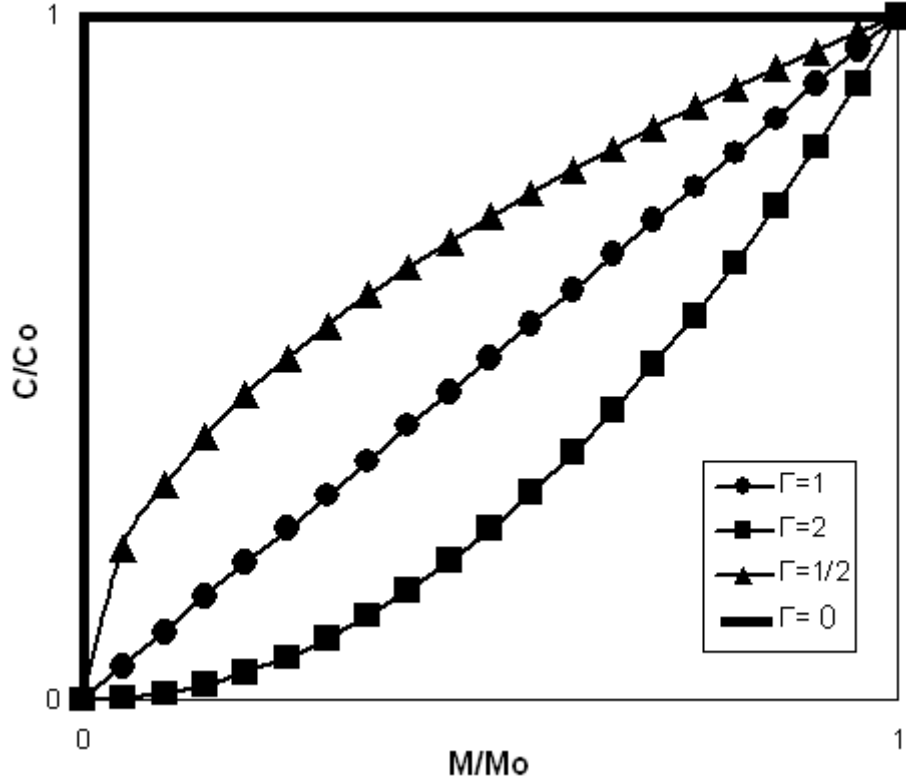


Figure 4.2. Plots of the source power function for varying values of Γ .

calculate the source mass and discharge concentration during the experiment. The source mass at any time during the experiment is

$$M(t) = \left[\frac{-QC_0}{\lambda_s M_0^\Gamma} + \left(M_0^{1-\Gamma} + \frac{QC_0}{\lambda_s M_0^\Gamma} \right) e^{(\Gamma-1)\lambda_s t} \right]^{\frac{1}{1-\Gamma}} \quad (4.4)$$

and the concentration of the water leaving the source zone is

$$C_s(t) = \frac{C_0}{M_0^\Gamma} \left[\frac{-QC_0}{\lambda_s M_0^\Gamma} + \left(M_0^{1-\Gamma} + \frac{QC_0}{\lambda_s M_0^\Gamma} \right) e^{(\Gamma-1)\lambda_s t} \right]^{\frac{\Gamma}{1-\Gamma}} \quad (4.5)$$

One special condition for the source equation occurs when $\Gamma = 1$. This produces a situation where the source mass and the concentration leaving the source zone decrease at

the same rate. Simplifying Equation (4.3) for $\Gamma = 1$ results in an exponential function for the decrease of mass and concentration over time. The solution for mass with $\Gamma = 1$ is

$$M(t) = M_0 e^{-\left(\frac{QC_0}{M_0} + \lambda_s\right)t} \quad (4.6)$$

and similarly the concentration leaving the source zone is

$$C_s(t) = C_0 e^{-\left(\frac{QC_0}{M_0} + \lambda_s\right)t} \quad (4.7)$$

With this scenario, the source mass experiences first-order exponential decay. It decreases rapidly at first and less rapidly at later times, and the source mass never reaches zero. This results in a high initial discharge with extensive tailing (Parker and Park, 2004; Falta et al., 2005; Newell and Adamson, 2005). This approximation for modeling the decay of source mass is sometimes considered the “middle-of-the-road” approach, and is a reasonable assumption for planning level models (Newell and Adamson, 2005).

Another special condition occurs when $\Gamma = 0$. This is a step-wise solution, meaning that the concentration leaving the source zone is constant ($C_s = C_0$) until the source is completely depleted. To find the mass in source zone for this case Equation (4.3) is solved using $\Gamma = 0$. The mass in the source zone at any time for the case where $\Gamma = 0$ is found by

$$M(t) = \frac{(M_0 \lambda_s + QC_0) e^{-\lambda_s t} - QC_0}{\lambda_s} \quad (4.8)$$

To find the time when the source mass will be completely depleted Equation (4.8) is solved using $M(t) = 0$. The source zone mass will be completely depleted at a time of

$$t = -\frac{1}{\lambda_s} \ln \left(\frac{QC_0}{QC_0 + \lambda_s M_0} \right) \quad (4.9)$$

For a small initial mass this condition is similar to an instantaneous source term, where mass in the source zone is immediately flushed downgradient (Falta et al., 2007). A conceptual model of instantaneous transport simulated using $\Gamma = 0$ is shown in Figure 4.3. The mass is flushed out of the source zone, and once the source has been depleted the mass moves downgradient as a pulse.

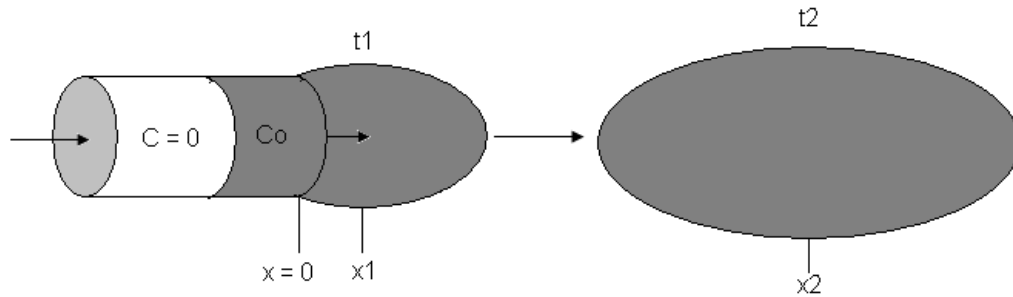


Figure 4.3. Conceptual model of instantaneous transport in REMChlor, where $\Gamma = 0$.

The source model in REMChlor also allows for source removal by some method other than dissolution and natural decay. This accommodates for models at sites where aggressive source remediation/ removal is proposed. Given the percentage of mass removed from the source over a period of time, the above mass and concentration equations are simply rescaled to adjust for the fraction of mass removed (X) for the remediation time (between t_1 and t_2). The specific equations for source remediation are included in Falta (2008).

4.1.2 Plume Model

A contaminant plume forms from mass in the source spreading downgradient. REMChlor uses an advection-dispersion equation to describe solute transport in the plume zone. The model includes first order decay reactions and retardation of the solute by adsorption. The current approach assumes that the pore-water velocity is constant in the longitudinal (x) direction, and considers scale dependent dispersion in the longitudinal, transverse and vertical directions. The governing equation for solute transport in the plume is

$$R \frac{\partial C}{\partial t} = -v \frac{\partial C}{\partial x} + \alpha_x v \frac{\partial^2 C}{\partial x^2} + \alpha_y v \frac{\partial^2 C}{\partial y^2} + \alpha_z v \frac{\partial^2 C}{\partial z^2} + rxn(x,t) \quad (4.10)$$

where C is the dissolved concentration of the chemical. The dispersivities are α_x , α_y , and α_z , where the subscripts refer to the direction of dispersion: x – longitudinal, y – transverse, and z – vertical. R is the retardation factor, and $rxn(x,t)$ accounts for destruction or generation of the species due to chemical or biological reactions. REMChlor allows the reaction rates to be functions of time and distance from the source (Falta, 2008).

The plume is coupled to the source zone mass balance given by Equation (4.1) combined with the rate of depletion power function, Equation (4.2). The mass flux entering the plume is from dissolved mass in the source (with a concentration of C_s) being flushed downgradient. The mass flux is expressed as

$$\frac{Q(t)C_s(t)}{A} = \left[\theta v C(t) - \theta \alpha_x v \frac{\partial C(t)}{\partial x} \right]_{x=0} \quad (4.11)$$

where θ is the porosity and Q is volumetric flow rate of water entering the plume region. A represents the cross-sectional area perpendicular to flow set at $x=0$, where the contaminant flux passes from the source to the plume. For areas below the water table $Q = \theta v A$.

The analytical solution to Equation (4.10) with variable decay rates is quite complex, so to simplify the solution a streamtube model is used. For this approach advection and reactions are separated from longitudinal dispersion, which is approximated by using a series of streamtubes with normally distributed pore velocity (Falta, 2008). Domenico's (1987) approximation is used to simulate transverse and vertical dispersion.

The concentration flux at the edge of the source boundary ($x = 0$) is calculated from Equation (4.11) using a streamtube with constant pore-velocity. Below the water table this simplifies to

$$C(t)|_{x=0} = C_s(t) \quad (4.12)$$

where the boundary condition is simply the time-dependent concentration in the source zone.

Transport within each streamtube is due only to advection. The advection front moves at a rate of v/R , so that at any time, the advection front is located at $x = tv/R$. The time it takes for the advection front to reach x is then $t_{travel} = Rx/v$. A parcel of water that reaches a specific location behind the front (x,t) was released from the source at

$$t_{release} = t - Rx / v \quad (4.13)$$

where t is the total time. This leads to a concentration at (x,t) of

$$C(x, t) = C(t_{release})|_{x=0} \quad (4.14)$$

With first order decay taking place within the plume, the concentration then becomes

$$C(x, t) = C(t - Rx/v)|_{x=0} \exp\left(\frac{-kx}{v}\right) \quad (4.15)$$

where k is the rate of a first-order reaction (Falta, 2008).

Longitudinal dispersion is included in the plume model by using a bundle of streamtubes with a normally distributed velocity field. The velocity field has a mean velocity of \bar{v} and a standard deviation of σ_v . For a specific location (x,t), a velocity of v^* is needed for the advection front to reach that exact point. The overall concentration as a function of distance and time comes from the probability that a streamtube's velocity (v) is less than v^* . The normalized concentration is expressed as

$$\frac{C}{C_0} = \frac{1}{2} \operatorname{erfc}\left(\frac{x - \bar{v}t}{\sigma_v t \sqrt{2}}\right) \quad (4.16)$$

This has the same form as the 1-D advection-dispersion equation for an infinite system

$$\frac{C}{C_0} = \frac{1}{2} \operatorname{erfc}\left(\frac{x - \bar{v}t}{2\sqrt{\alpha_x \bar{v}t}}\right) \quad (4.17)$$

These equations are the same when the dispersivity in Equation (4.17) is

$$\alpha_x = \frac{\sigma_v^2}{2\bar{v}} t = \frac{\sigma_v^2}{2\bar{v}^2} \bar{x} = a\bar{x} \quad (4.18)$$

where \bar{x} is the average location of the advective front ($\bar{x} = \bar{v}t$). Therefore, the streamtube method produces scale-dependent longitudinal dispersion, where the

dispersivity is a linear function of distance and $a = \frac{\sigma_v^2}{2\bar{v}^2}$ (Falta, 2008).

The streamtube model is constructed in REMChlor using a specified number of streamtubes, n , and the maximum and minimum velocities (v_{\max} , v_{\min}) for the system.

The range of velocity for the streamtubes is

$$\Delta v = \frac{v_{\max} - v_{\min}}{n} \quad (4.19)$$

Each streamtube is assigned a weight, based on the probability that it is within the range

of $v - \frac{\Delta v}{2} < v < v + \frac{\Delta v}{2}$. The solution for transport with longitudinal dispersion is found

by first solving the analytical solution for advection of each streamtube with reaction and applying the weight found above to each streamtube. The sum of the weighted concentrations for each streamtube gives $C(x,t)$ (Falta, 2008).

Transverse (y) and vertical (z) dispersion are included by using the Domenico (1987) approximation. This produces 3-D dispersion from the case where only longitudinal dispersion was considered:

$$C(x, y, z, t) = C(x, t) f_y(y) f_z(z) \quad (4.20)$$

The functions from Domenico's approximation are

$$f_y(y) = \frac{1}{2} \left(\operatorname{erf} \left\{ \frac{y + Y/2}{2\sqrt{\alpha_y x}} \right\} - \operatorname{erf} \left\{ \frac{y - Y/2}{2\sqrt{\alpha_y x}} \right\} \right) \quad (4.21)$$

for dispersion in the transverse direction and

$$f_z(z) = \frac{1}{2} \left(\operatorname{erf} \left\{ \frac{z + Z}{2\sqrt{\alpha_z x}} \right\} - \operatorname{erf} \left\{ \frac{z - Z}{2\sqrt{\alpha_z x}} \right\} \right) \quad (4.22)$$

for the vertical direction. There is some error associated with Domenico's approximation, but it will be small for small values of dispersion (Domenico, 1987).

REMChlor allows reaction rates to vary in both time and space for the plume zone. This helps simulate remediation techniques for organic contaminants where reaction rates are manipulated to further contaminant decay.

REMChlor also accounts for parent-daughter reactions. Transport of up to 4 components is calculated for the plume region. The daughter products are coupled to the parent compound by the yield coefficients and rate constants (Falta et al., 2007).

CHAPTER 5

REMCHLOR SIMULATIONS

The REMChlor model was used to simulate tritium transport during the MADE-2 experiment. Two simulations were conducted. The first simulation aims at representing classical tritium transport for an instantaneous source. The goal of the second simulation was to reproduce the tritium distributions observed during MADE-2.

REMChlor uses units of mass for the amount of contaminant in the system. In the case of tritium and other radioactive solutes, radioactivity is a more suitable unit of measurement. For a radioactive element, activity is related to mass, and the activity concentration (activity per volume) relates to the mass concentration. This study of tritium is conducted in units of activity, and conventional terms of mass and concentration are used interchangeably to describe the activity of tritium.

5.1 Classical transport

The MADE-2 experiment was set up as an instantaneous source contaminant transport test. The tracer solution, containing tritium, was injected into the subsurface over two days, which is relatively instantaneous compared to the time-span of the experiment – about one year. Because tritium is a conservative tracer, it would be expected to move downgradient as a pulse without reacting with the aquifer materials.

REMChlor divides the aquifer system into two separate zones, the source and plume. To model contaminant transport in an aquifer using REMChlor, the first step must be to define the source and the plume zone.

5.1.1 Source Zone

In REMChlor, an instantaneous source scenario is approximated by assigning the source decay exponent (Γ) a value of 0. This treats the source zone like a plug flow reactor, where the concentration leaving the source zone is constant until the source is completely depleted (Figure 4.3). The mass in the source zone for this case where $\Gamma = 0$ is calculated using Equation (4.8)

The initial amount of tritium in the source zone (M_0) is the total activity of the tritium injected into the aquifer for the experiment. The injected mass had an activity of 0.5387 Ci. The initial concentration leaving the source zone (C_0) is harder to estimate. The value of C_0 is the flow averaged concentration of tracer crossing the source – plume boundary at the initial time. To find C_0 the spatial extent of the source zone needs to be defined and the concentration crossing the plane that divides the source and plume zones should be measured. Figure 5.1 shows a conceptual model of the source zone. The source – plume boundary is at $x = 0$, and C_0 is the concentration at the boundary for time zero.

The source zone for this simulation of classical tritium transport was defined to be the immediate area of the injection wells. The downgradient plane was set to a width of 4 m for the five injection wells spaced 1 m apart. The vertical extent of the source zone is 7 m. The plane was set at a distance about 3 m downgradient of the injection wells. The

source-plume boundary was defined to be immediately downgradient of the injection wells for this case because this simulation aims to approximate classical tritium transport for an instantaneous source. The boundary is located at 3 m because the nearest sampling points to the injection site are between 2 and 3 m downgradient of the injection wells.

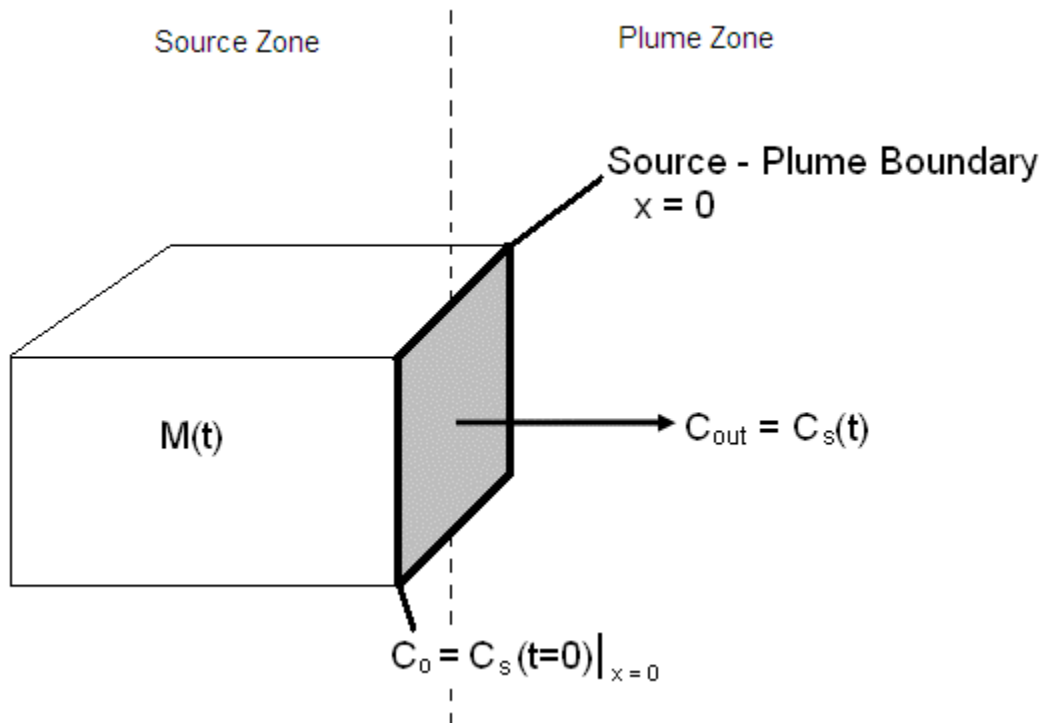


Figure 5.1. Conceptual model of the source zone.

For the MADE-2 experiment the first measurements were taken 27 days after injection. This is the first time period that data are available downgradient of the injection wells. For the purpose of determining C_0 the measurements at day 27 are used to approximate the initial concentration at time zero.

The concentration measurements at the source-plume boundary approximately 3 m downgradient of the injection wells were used to find C_0 . There are two wells at the defined source – plume boundary, and measurements were taken at several depths in these two wells. These wells have x – y coordinates of (2.1, 0.3) and (2.9, 2.1) m. The concentration measurements from these wells at the snapshot at day 27 were spatially averaged to determine C_0 .

The weighted average was determined by first assigning a local area to each sampling point. A rectangular grid perpendicular to the direction of flow was used, with the sampling point at the center of the grid. The width of each rectangle was given a length equal to the distance between the two sampling wells, about 2 m. The length of each rectangle considers the distance between the points above and below each sampling point. One-half the distance between the sampling point and the one immediately above or below it is the distance between the sampling point and the top or bottom of the rectangle, respectively. The area of the rectangle associated with each sampling point is the width multiplied by the sum of the distance above and below the point. Figure 5.2 shows a diagram of the area associated with the sampling points.

Because C_0 represents the flow averaged concentration leaving the source zone, the volumetric flow rate (Q) across the area assigned to each sampling point is considered. The volumetric flow rate associated with each sampling point is the specific discharge, or Darcy velocity (v_d), across the area of each rectangular grid $Q = v_d A$. The volumetric discharge was used to find the mass discharge (D) for each area $D = CQ$, where C is the concentration at each sampling point.

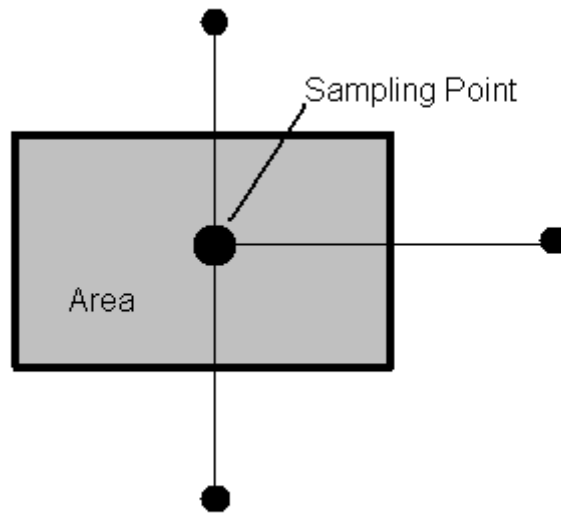


Figure 5.2. The area associated with the sampling point is shaded gray. The points above and below each sampling point are used to determine the height of the rectangle, and the point from the other well (to the right in this example) is used to determine the width of the block.

The averaged concentration for the boundary was found by dividing the sum of the mass discharges for each area by the sum of the volumetric discharges for each area.

$$C_0 = \frac{\sum D}{\sum Q} \quad (5.1)$$

The average concentration at this plane, about 3 m downgradient of the injection wells at 27 days, is 10^4 pCi/mL.

The source mass is depleted by two processes. The dominant process is flushing, where clean water flowing through the source zone flushes contaminant downgradient. The discharge of mass into the plume is determined by the volumetric flow rate out of the

source zone. The other process that contributes to source depletion is radioactive decay of tritium. Tritium has a half-life of 12.32 years, which gives it a first-order decay rate of 0.055 yr^{-1} .

5.1.2 Plume Zone

In REMChlor, the plume zone is modeled using classical advection – dispersion including solute retardation and decay. Most of these parameters are based on physical information and can be estimate from the tested aquifer properties and knowledge about the solute.

REMChlor requires that the Darcy velocity be constant for the spatial extent of the model. The Darcy velocity of the flow leaving the source zone is the same Darcy velocity used for transport in the plume zone. The pore velocity (v) is related to the Darcy velocity (v_d) by the porosity (θ) of the medium

$$v = \frac{v_d}{\theta} \quad (5.2)$$

The value for the Darcy velocity used in the model was calculated from Equation (5.2), using the observed pore velocity. The average porosity at the MADE site was measured at 31%, but 35% is used to account for compaction that may have occurred during sampling (Adams and Gelhar, 1992).

The pore velocity used to calculate v_d was estimated from the velocity of the leading edge of the plume during the MADE-2 experiment. The velocity of the leading edge of the plume was found by calculating the distance traveled by the leading edge during each time period. Table 5.1 shows the maximum distance the plume reached at

each sampling snapshot and the velocity of the tracer for the time leading up to each snapshot. The average velocity of the leading edge of the tritium plume was 274 m/yr, which gives an average Darcy velocity value of 95.9 m/yr. A Darcy velocity of 100 m/yr was used in the model.

Time [days]	X [m]	V [m/d]
27	25	0.93
132	70	0.43
224	230	1.7
328	250	0.19

Table 5.1. The maximum distance reached by the leading edge of the plume at each sampling snapshot. The velocity of the leading edge was calculated for the time leading up to each time step.

REMChlor considers solute dispersion in three dimensions. The value of longitudinal dispersivity used in several models of the tritium tracer experiment at MADE-2 varies between 10 m (Boggs et al., 1993) and 1 m (Feehley et al., 2000; Guan, 2006). In a modeling study of the MADE site conducted by Feehley et al. (2000) the ratio of transverse to longitudinal dispersivity was set at 0.01, and the ratio of vertical to longitudinal dispersivity was set at 0.001. These values were used to correspond with limited transverse and vertical dispersivity seen at the MADE site (Feehley et al., 2000; Guan et al., 2008).

Longitudinal dispersion is included in REMChlor by using a bundle of streamtubes with a normally distributed velocity. The input for longitudinal dispersion in REMChlor is the coefficient of variation ($\Sigma_v = \sigma_v / \bar{v}$) of the normally distributed velocity

field. Longitudinal dispersivity is related to Σ_v by $\alpha_x = \frac{1}{2} \Sigma_v^2 \bar{x}$, where \bar{x} is the average location of the advective front (Falta, 2008). This approach to longitudinal dispersion produces scale dependent dispersion that increases with distance. Using a σ_v value of 0.2 produces a longitudinal dispersivity that is 1/50th of the travel distance. This gives α_x a value of 2 m at a distance 100 m downgradient, and at a distance of 300 m the value of α_x is 6 m. These values fall within the range of previous models. The ratios of transverse and vertical dispersivity to longitudinal dispersivity used in this study are 0.1 for transverse and 0.01 for vertical dispersivity. These values produced a plume that best matched the width and length of the observed tritium plume at the MADE site.

Aside from advection and dispersion, the only other mechanism occurring in the plume zone for tritium is radioactive decay. The first-order decay rate is constant for the source zone and the plume zone.

5.1.3 Results

Table 5.2 shows the input parameters used to simulate classical tritium transport for the physical properties at the MADE site. The simulations were run using 5000 streamtubes.

The calculated tritium concentration distributions are shown in Figure 5.3. These plots show a pulse of tritium that moves downstream of the injection wells. As the time after injection increases the pulse spreads out and moves further down stream. The spreading is due to dispersion and the time it takes to deplete the source zone. This time it takes the source mass to be depleted for this case, where $\Gamma = 0$, is calculated from

Equation (4.9). Using the values presented in Table 5.2, the source mass will be depleted 7 days after the injection period. The time period over which the source mass is flushed into the plume zone contributes to the elongation of the plume shown in Figure 5.3. At the last snapshot at 328 days, the leading edge of the pulse has traveled beyond 300 m and is cut off by the downgradient edge of the model domain, which corresponds to the end of the sampling network.

Source Parameters		
M_0	C_i	0.5387
C_0	pCi / mL	10,000
Gamma	---	0
Source Width	m	4
Source Depth	m	7
v_d	m / yr	100
Decay	1 / yr	0.055
Plume Parameters		
Porosity	---	0.35
α_x	---	0.02 x
α_y	---	0.002 x
α_z	---	0.0002 x

Table 5.2. Input parameters used to simulate classical tritium transport.

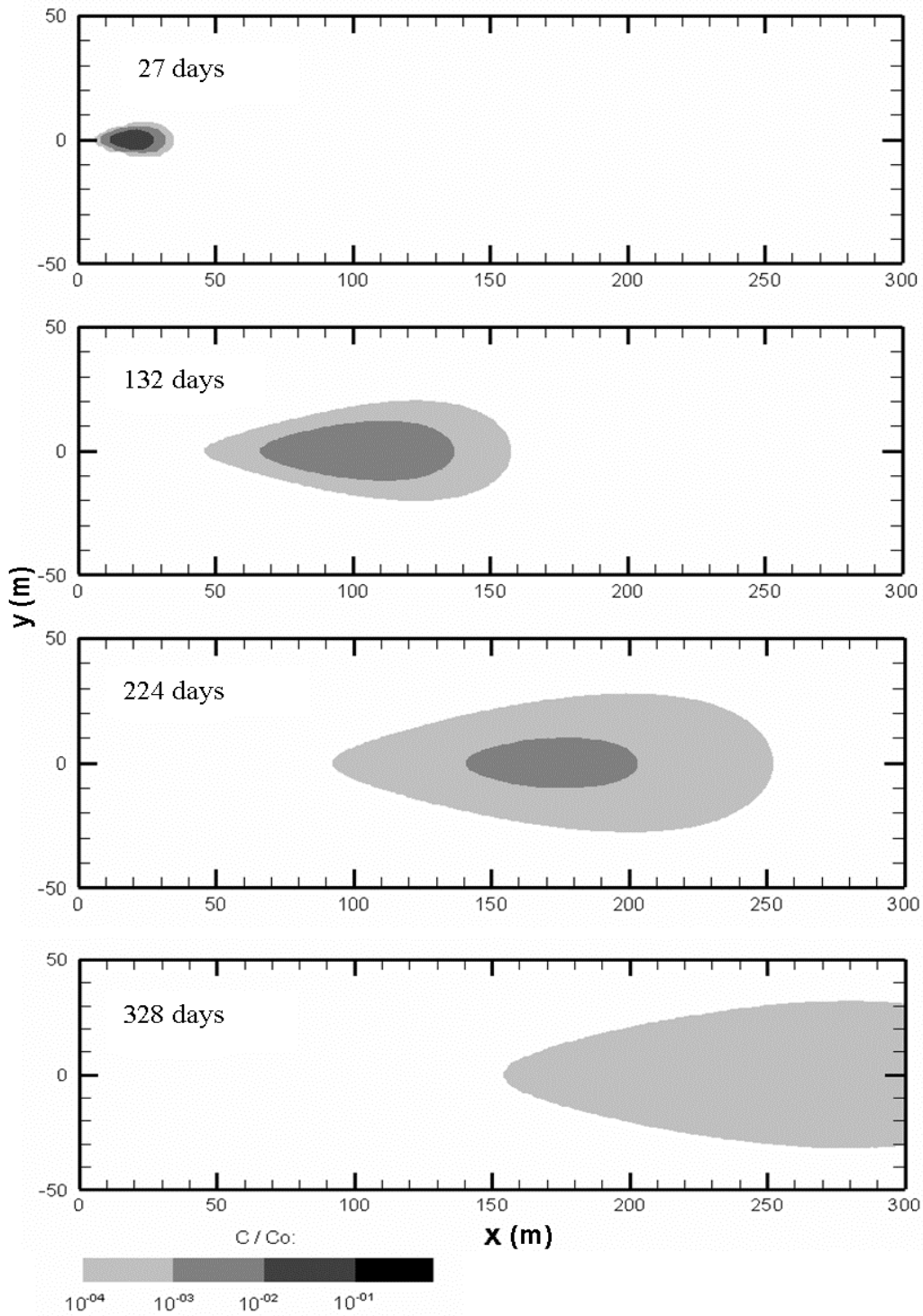


Figure 5.3. Classical tritium transport for an instantaneous source. The solute travels downstream as a dispersing pulse.

5.1.4 Mass Distributions

The mass distributions of tritium produced by the REMChlor simulations are compared to the data. The site was divided into 6 zones along the longitudinal (x) axis of the plume to show the amount of tritium in each zone. Each zone represents 50 m of length, and the range covered by each zone is shown in Table 5.3. The mass distributions from the MADE-2 experiment were taken from Guan (2006).

Zone	1	2	3	4	5	6
Range (m)	0 - 50	50 - 100	100 - 150	150 - 200	200 - 250	250 - 300

Table 5.3. The range along the longitudinal (x) axis covered by each zone for the mass distribution plots.

The mass distributions at MADE-2 were found by the spatial moments analysis on the data from the tritium tracer test. In the spatial moments study included in Boggs et al. (1993), the total sampled mass was calculated using the zeroth moment. Equation (3.1) shows the formula for the zeroth moment. The results of the spatial moments analysis are shown in Table 3.1 for the entire network of sampling points.

The mass distributions of the tritium data at MADE-2 across 6 – 50 m long zones were found the same way as the total mass for the entire domain. The data points were grouped into zones based on its distance from the injection wells ($x = 0$ m). The zeroth moment calculation was then performed on each of these sub-domains to determine the total mass in each zone (Guan, 2006).

The calculated mass distributions for the current simulations utilize the REMChlor output files. REMChlor produces a mass discharge output file for each

simulation that is run with the program. The mass discharge (units of Mass / Time) file shows the amount of mass crossing the plane at each x-interval over time. Figure 5.4 is a schematic for the setup of the mass discharge output file from REMChlor. The mass discharge is shown leaving the plane at each x-interval.

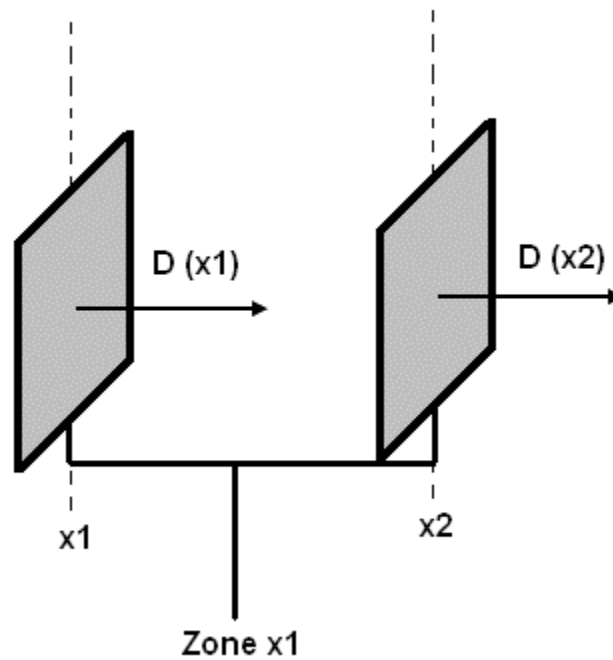


Figure 5.4. The mass discharge output file gives the mass discharge (D) across each plane at the x -intervals.

The mass discharge data were numerically integrated by time to find the total mass leaving each plane. Each integration was calculated starting from time = 0. The integrations for each snapshot were run using 50 time intervals leading up to the time of the snapshot. The trapezoidal rule for numerical integration was used to integrate the mass discharge data. The mass for each time interval, between t_1 and t_2 , was calculated

by $M(t_2) = \frac{1}{2}(D(t_2) + D(t_1))(t_2 - t_1)$. The calculated masses for each time interval were summed to get the total mass crossing each x-interval plane over the given time interval.

The mass in each zone is equal to the cumulative mass entering the zone minus the mass leaving the zone at the downgradient plane. In Figure 5.4 the mass in zone x1 is equal to the integral of the mass entering the zone, calculated at x1, minus the integral of the mass leaving the zone, calculated at x2.

The REMChlor output file shows the distribution of mass in the plume zone. While REMChlor internally calculates the mass remaining in the source zone, the output files do not include the remaining mass in the source zone. This analysis considers the distribution of the total tritium activity, so the mass remaining in the source zone needs to be calculated separately. The change in mass in the source zone is based on the conservation of mass coupled with the power function relating discharge concentration to mass (Γ). The mass in the source zone at any time for any value of Γ is shown by Equation (4.4) (Falta et al., 2005). In this simulation where the goal was to produce the results of classical tritium transport Γ was given a value of 0 to simulate an instantaneous source. For a Γ value of 0 Equation (4.4) was simplified to Equation (4.8), so that the mass remaining in the source zone for this case is

$$M(t) = \frac{(M_0\lambda_s + QC_0)e^{-\lambda_s t} - QC_0}{\lambda_s} \quad (5.3)$$

The source mass is included with the mass in the first zone. The first zone ranges from 0 – 50 m downgradient of the injection wells; x = 0 m is the location of the injection

wells. In this case the source – plume boundary is considered to be immediately downstream of the injection wells.

Equation (4.9) showed the time it takes for the source mass to be completely depleted for the case where $\Gamma = 0$.

$$t = -\frac{1}{\lambda_s} \ln \left(\frac{QC_0}{QC_0 + \lambda_s M_0} \right) \quad (5.4)$$

Solving this equation with the values used in the classical model, shown in Table 5.2, gives the time that all of the tritium in the source should have been flushed downgradient into the plume zone. For the parameters used in the classical model the source should have been depleted 7 days after the start of the experiment. For this case the source would have no tritium tracer left in it at the first sampling snapshot at 27 days, so source mass would not contribute to the distribution of mass at times greater than 7 days.

Figure 5.5 shows the distribution of mass for the tritium tracer test at MADE-2 compared to the calculated mass distributions of tritium tracer for the classical model. The mass has been normalized to the total activity of the injected tracer, so that the values of mass represent the fraction of the initial mass in each zone. With the tritium data from the MADE-2 experiment the majority of the mass remains in the first zone, less than 50 m downgradient of the injection wells, for the duration of the experiment. By the end of the experiment at 328 days, over 50% of the injected mass was still in the first zone. The classical model, however, shows a pulse that moves downgradient of the injection wells. With increasing time the peak has moved further downgradient, so that the peak is in the

first, third, fourth and sixth zone at 27, 132, 224, and 328 days, respectively. At the last snapshot the tritium pulse extends beyond 300 m.

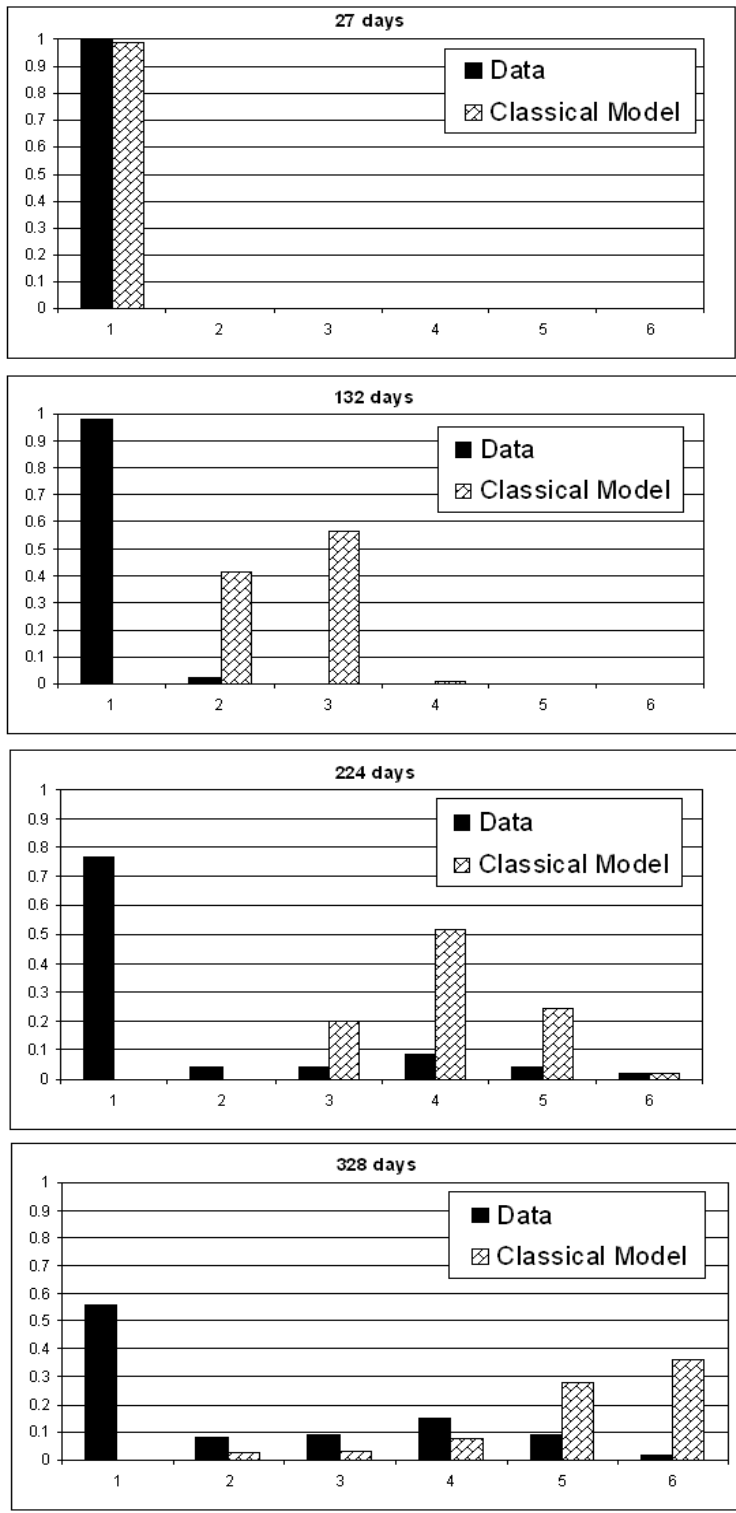


Figure 5.5. Distribution of tritium tracer into zones 50 m long.

5.2 Souce – Plume Model

The tritium distributions during the MADE-2 experiment do not look like the pulse that is expected for classical transport. Rather, the distributions at the site show a non-Gaussian distribution, with high concentrations remaining near the injection wells and a low concentration leading edge extending downgradient. These distributions resemble those seen at sites with NAPL contamination. This suggests that the REMChlor model, designed for NAPL contaminated sites, could be used to reproduce the tritium distributions at MADE-2.

The source zone in REMChlor acts as a reservoir for the tracer, which it releases to the plume zone. The rate the tracer is released into the plume zone is determined by the flow rate through the source zone (Q) and the relationship between discharge and mass, characterized by Γ .

5.2.1 Parameters

The mass in the source zone is gradually decreasing at the MADE site. A reasonable estimate for overall source decay is to assume that the decrease in source mass and the concentration of tracer leaving the source zone have a 1 to 1 relationship so that they decrease exponentially (Falta et al., 2005; Newell and Adamson, 2005). The 1 to 1 relationship is used in this study. This is done in REMChlor by using a Γ value of 1.

The source zone was defined using information from the measurements taken at the first snapshot (27 days after injection) during MADE-2. Figure 5.6 shows the tritium distributions at the final snapshot for the experiment, 328 days after injection. This shows that the maximum concentration remains within 20 m of the injection wells. The

source zone is defined as being 20 m wide to match the apparent width of the source zone in Figure 5.6. The depth is the same as used for the classical model, 7 m.

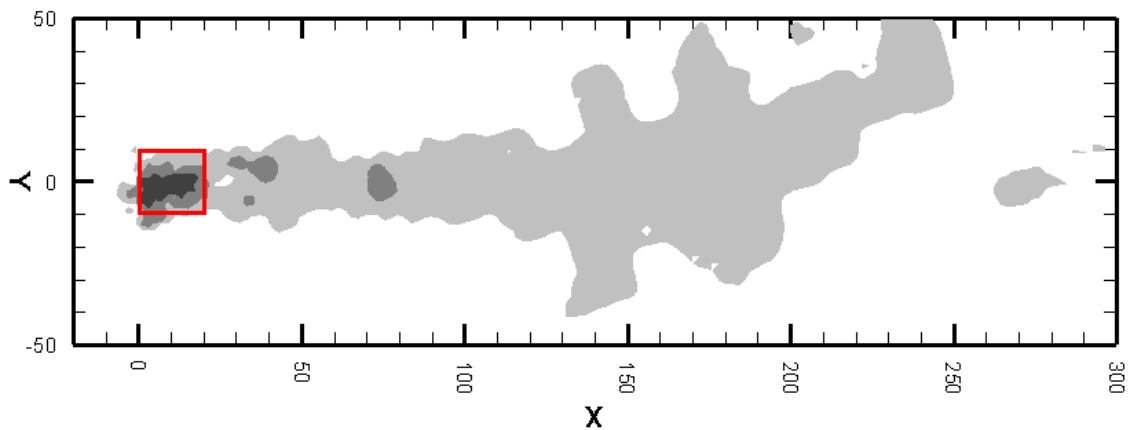


Figure 5.6. Plot of the tritium concentration distributions for the snapshot at 328 days at MADE-2. A box is drawn around the area defined as the source zone. The boundary separating the source from the plume zone is the downgradient side, the right side, of the box.

The initial concentration leaving the source zone was estimated using the concentration values downgradient of the injection wells near the plane used to define the source – plume boundary. This approximation assumes that the concentration from the points near the plane is constant over the entire width of the plane.

The area extending approximately 20 m downgradient of the injection wells was defined as the source zone, so that the plane separating the source and plume zones should be situated at about 20 m. The initial concentration crossing the source – plume boundary is found from the data of concentration measurements collected at 27 days. The measured concentrations at MADE-2 for the snapshot at day 27 vary by three orders of magnitude between 15 and 20 m from the injection wells.

The concentration measurements within the range of 15 to 20 m downgradient of the injection wells were considered for estimating the best value of C_o for the MADE-2 experiment. Several concentration measurements were taken from different depths for each sampling well, with specified $x - y$ coordinates. The concentrations along the depth of each well were vertically averaged to find the average concentration for the $x - y$ location of each well. The spatial averaging was performed using the same procedure described to get the initial source concentration for the classical model, with the exception that the distance between other sampling wells is not considered (the concentration is only averaged with regard to the vertical extent of the measurements for each sampling well).

The concentration measurements were flow averaged for the local area associated with each sampling point along the depth of the well. The volumetric flow rate (Q) across each area was found by multiplying the area by the Darcy velocity. The mass discharge (D) was found by multiplying the concentration at each sampling point by Q . The sums of volumetric flow rate and mass discharge at each sampling point were calculated for each sampling well. The average concentration at each sampling well is the sum of D divided by the sum of Q .

Figure 5.7 shows the vertically averaged values of concentration (pCi/mL) calculated at each sampling well that falls within the range of 15 to 20 m downgradient of the injection site ($x = 0$ m). The concentration varies by 3 orders of magnitude down the centerline (where $y = 0$ m). The dashed lines represent possible source-boundary planes.

The location on the x-axis of each plane was based on the order of magnitude of the calculated concentrations near the centerline.

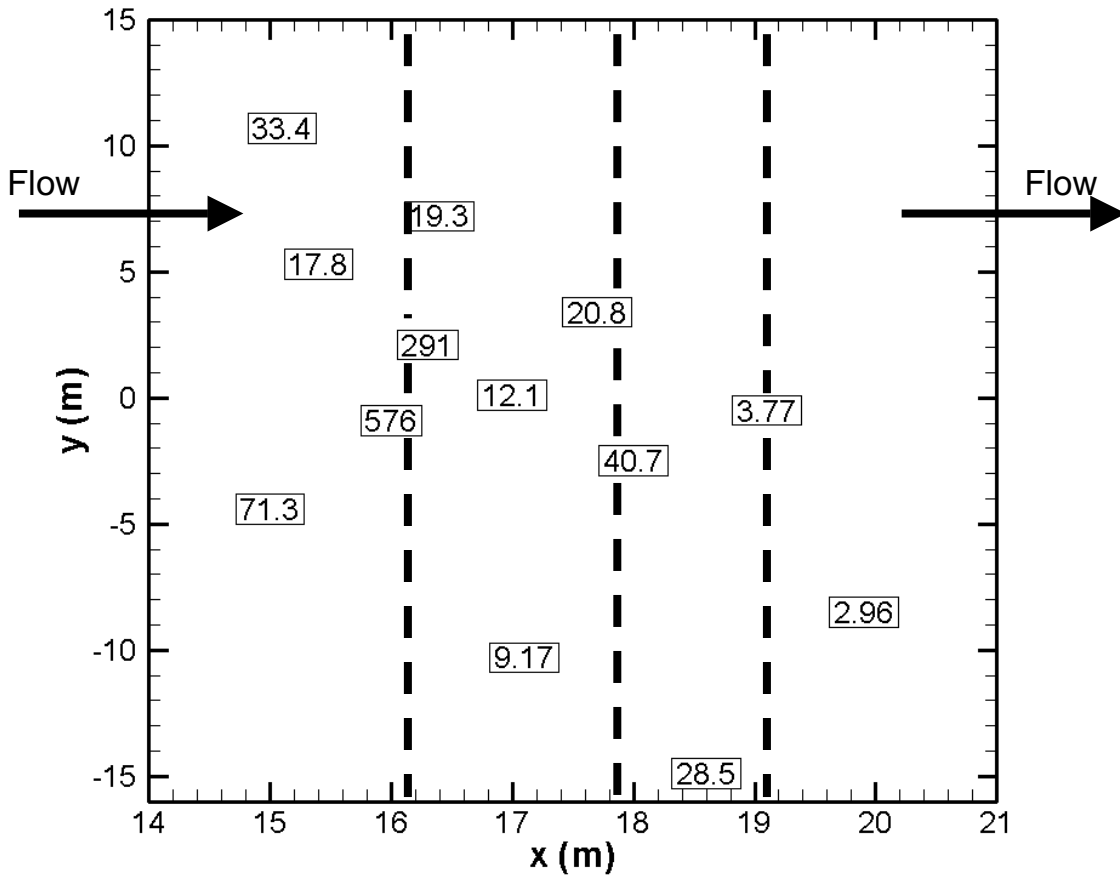


Figure 5.7. Vertically averaged values of concentration (pCi/mL) measured at 27 days for the sampling wells located 15 – 20 m downgradient of the injection wells. The dashed lines highlight the range of concentrations near the centerline ($y = 0$ m) of the tritium distributions.

It is unclear which range of concentration should be used to define the source – plume boundary. To determine which value of C_0 reproduces the tritium distributions seen at the MADE site, three simulations were run with a different value of C_0 . The

three values of C_0 used were 4, 40, and 400 pCi/mL. These are reasonable approximations based on the concentrations shown in Figure 5.7.

The source – plume boundary is defined as being 20 m downgradient of the injection wells. This is an approximation based on the apparent size of the source zone (Figure 5.6). The estimates of C_0 are based on the observed concentrations at about 16, 18, and 19 m downgradient of the injection site.

The plume zone for this simulation uses the same parameters as the classical transport model. The only difference in the input between the classical model and the source – plume approach are the parameters used to define the source zone. Table 5.4 shows the input parameters used to simulate the tritium distributions at MADE-2. The simulations were run using 1000 streamtubes.

Source Parameters		
M_0	Ci	0.5387
C_0	pCi / mL	4; 40; 400
Gamma	---	1
Source Width	m	20
Source Depth	m	7
v_d	m / yr	100
Decay	1 / yr	0.055
Plume Parameters		
Porosity	---	0.35
α_x	---	0.02 x
α_y	---	0.002 x
α_z	---	0.0002 x

Table 5.4. Parameters used to simulate tritium transport at the MADE-2 site.

5.2.2 Mass Distributions

The distribution of mass calculated for each simulation was compared with the mass distributions observed at MADE-2 for each sampling period. The distribution of mass is shown by dividing the site into six 50 m long zones. The observed mass distributions at the MADE site are the same as shown in Figure 5.5, taken from Guan (2006). The mass distributions for the simulations were calculated using the mass discharge output file generated in REMChlor, as described earlier.

The mass in each zone is calculated from the mass discharge file using the same method as described before for the classical model. The mass discharge across each x-interval plane was numerically integrated by time to find the total mass crossing that plane. The mass in each zone is equal to the mass entering the zone minus the mass leaving the zone at the downgradient plane (Figure 5.4).

The REMChlor output files show the mass discharge for the plume zone. The source mass needs to be included in the total mass distributions to compare them to the observed tritium distributions. The source in this case uses a source depletion exponent (Γ) of 1 to simulate exponential decay of the source mass. The mass in the source zone at any time for $\Gamma = 1$ can be found by solving Equation (4.3), where $M = M_0$ at zero time (Falta et al., 2005). This produces Equation (4.6), where the mass in the source zone at time for the case where $\Gamma = 1$ is

$$M(t) = M_0 e^{-\left(\frac{QC_0}{M_0} + \lambda_s\right)t} \quad (5.5)$$

The solution to Equation (5.5) using the values shown in Table 5.4 for the 4 different times of each sampling snapshot gives the mass remaining in the source zone at each snapshot.

The calculated mass in the source zone was added to the mass in the first zone that was calculated from the mass discharge output files. The REMChlor output files use the convention of setting the source – plume boundary at $x = 0$ m. For MADE-2, $x = 0$ is considered to be the location of the injection wells. For this case the source – plume boundary is set at 20 m downgradient of the injection wells. The different definition of $x = 0$ between MADE-2 and REMChlor needs to be accounted for. The x -coordinates of the values calculated using REMChlor are adjusted by 20 m to account for this. For the first 50 m zone, the first 20 m are occupied by the source zone, and the plume contributes the mass for the remaining 30 m.

Figure 5.8 compares the mass distributions calculated from the REMChlor mass discharge files for the 3 different values of C_0 with the observed distributions of the tritium data. At the first snapshot at 27 days all values of C_0 show that the mass remains within the first zone. As time increases, the differences in the simulation results for the different values of C_0 become more apparent.

The smallest value of C_0 (4 pCi/mL) shows that the majority of the mass remains in the first zone for the duration of the experiment. By the end of the experiment at 328 days this simulation shows 88% of the mass still in the first zone, while the data shows only 56% in the first zone. For these simulations where $\Gamma = 1$ the source mass and the

source concentration are linearly related. Because the initial concentration leaving the source is small the mass is held up in the source zone.

For the simulation with the largest value of C_0 (400 pCi/mL) the mass moves downgradient more quickly than it does in the field case. This resembles the tritium pulse that was calculated by the classical model in Figure 5.5. The initial concentration leaving the source zone and the flow rate across the source – plume boundary are high enough that the mass in the source zone decreases rapidly. At the first snapshot at 27 days the mass remaining in the source zone is already smaller than the amount of mass that has been flushed into the first zone.

The simulation that uses the median value of C_0 (40 pCi/mL) matches the data throughout the duration of the experiment better than the other two cases. This simulation produces mass that consistently moves downgradient with time. The simulated mass distributions match the observed mass distributions, and both the simulated and observed distributions follow the same trend. This suggests that a C_0 value of about 40 pCi/mL best describes the initial concentration leaving the source zone.

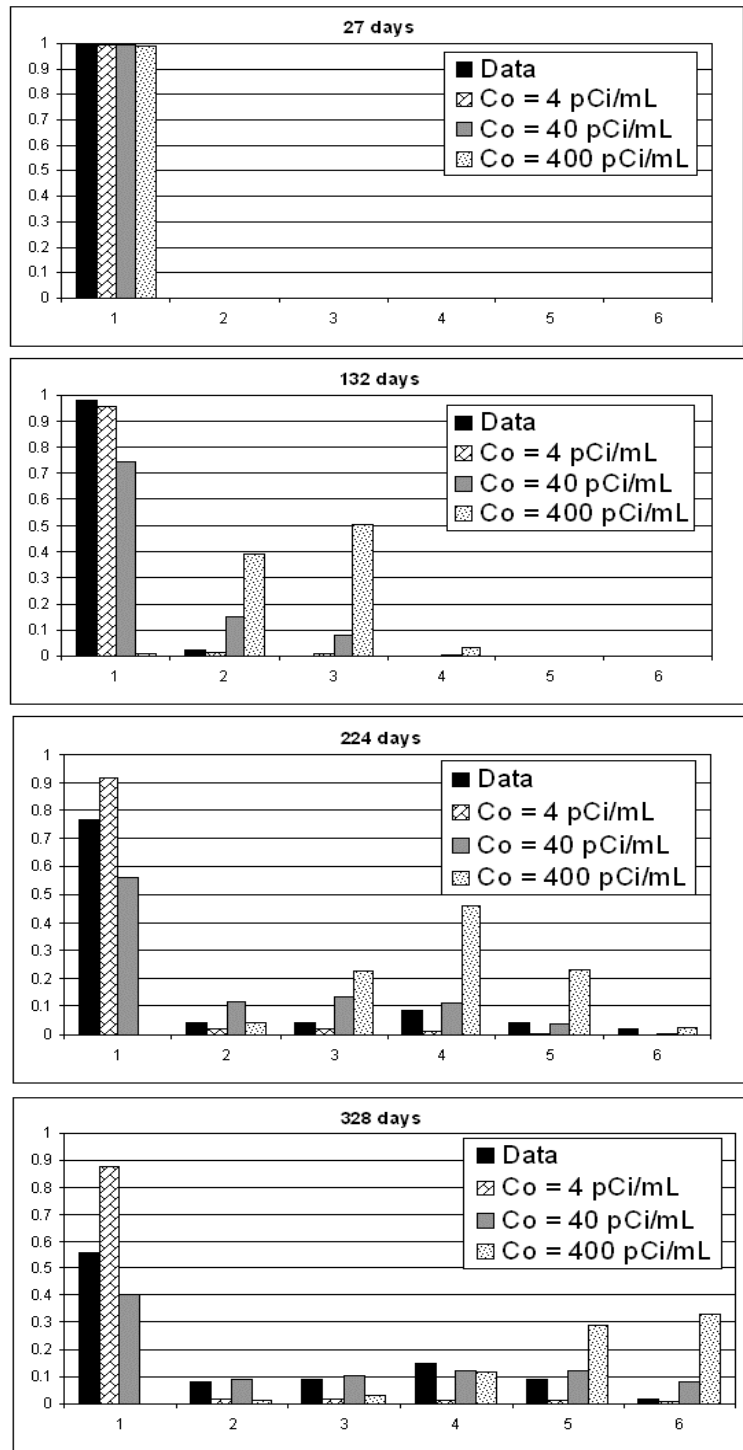


Figure 5.8. Mass distributions for the source - plume simulations in REMChlor for 3 different values of C_0 . The simulations are compared against the observed tritium distributions.

5.2.3 Concentration Distributions

The tritium concentration distributions were simulated using the values shown in Table 5.4. An initial concentration of 40 pCi/mL was used in REMChlor to simulate the concentration distributions, because this value produced mass distributions that best matched the observed mass distributions.

Contour plots of the tritium concentrations for the four sampling snapshots at 27, 132, 224 and 328 days are shown in Figure 5.9, Figure 5.10, Figure 5.11, and Figure 5.12, respectively. These plots compare the simulated tritium distributions with the observed distributions at MADE-2. The calculated concentration distributions match the observed distributions best at the later snapshots at 224 and 328 days. For the earlier snapshots the simulated concentration contours extend further downgradient than the observed concentrations.

The source zone in the simulated plots is shown as a box. The box has the same dimensions as the parameters used to define the source zone, and it extends 20 m downgradient of the injection wells. The tritium data collected during MADE-2 defines $x = 0$ as the location of the injection wells. As discussed previously, REMChlor considers the source – plume boundary to be $x = 0$. The simulated contour plots have been adjusted to agree with the convention that $x = 0$ is the injection site.

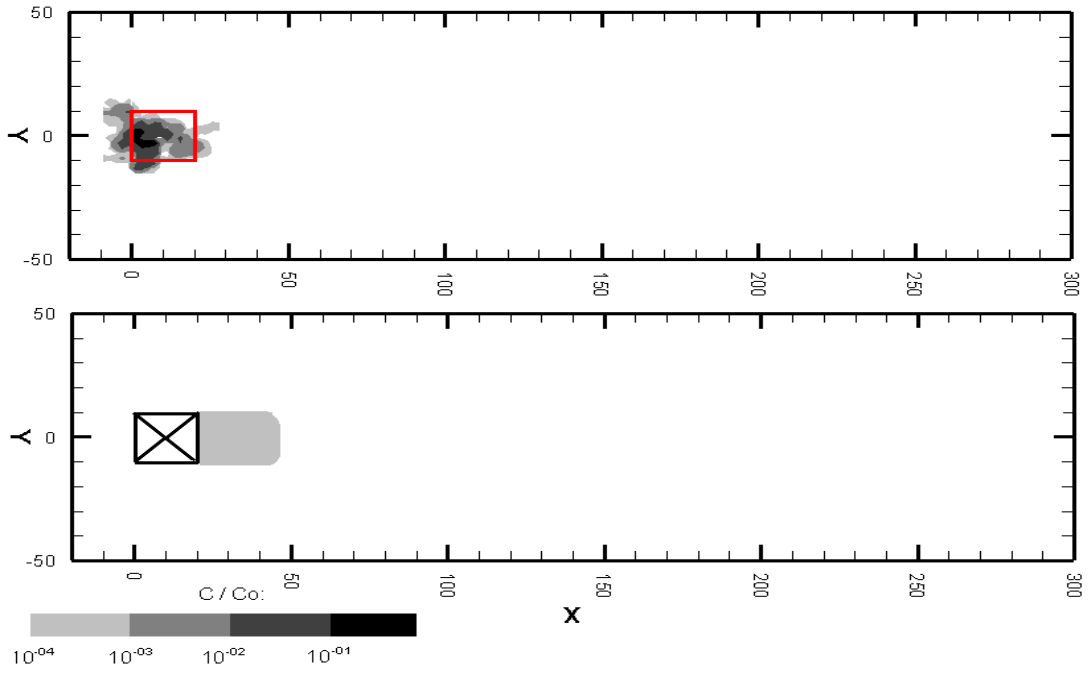


Figure 5.9. Results for 27 days. The tritium distributions of the data (top) are compared with the REMChlor simulation (bottom). The crossed box in the simulation plot represents the source zone.

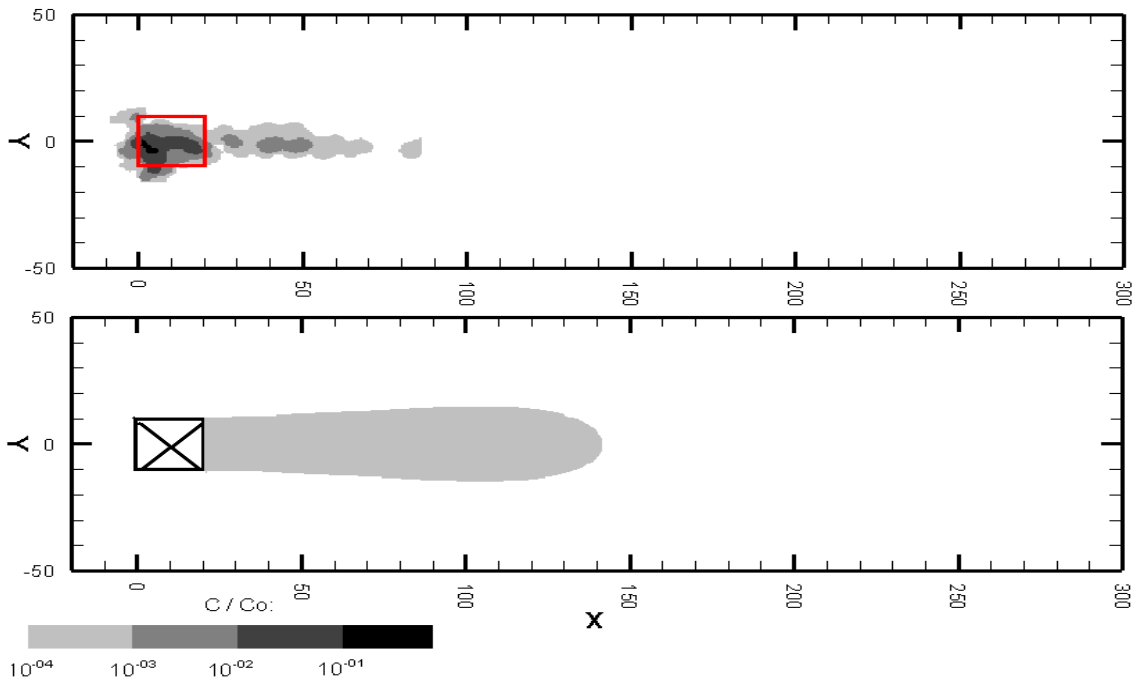


Figure 5.10. Results for 132 days.

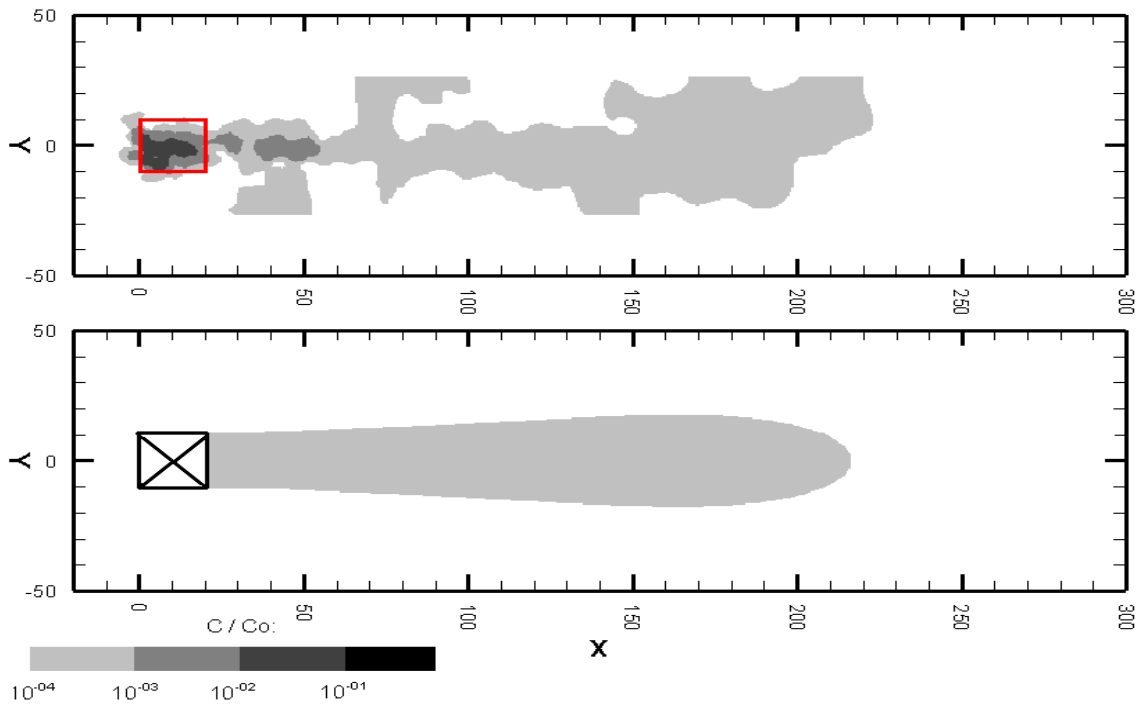


Figure 5.11. Results for 224 days.

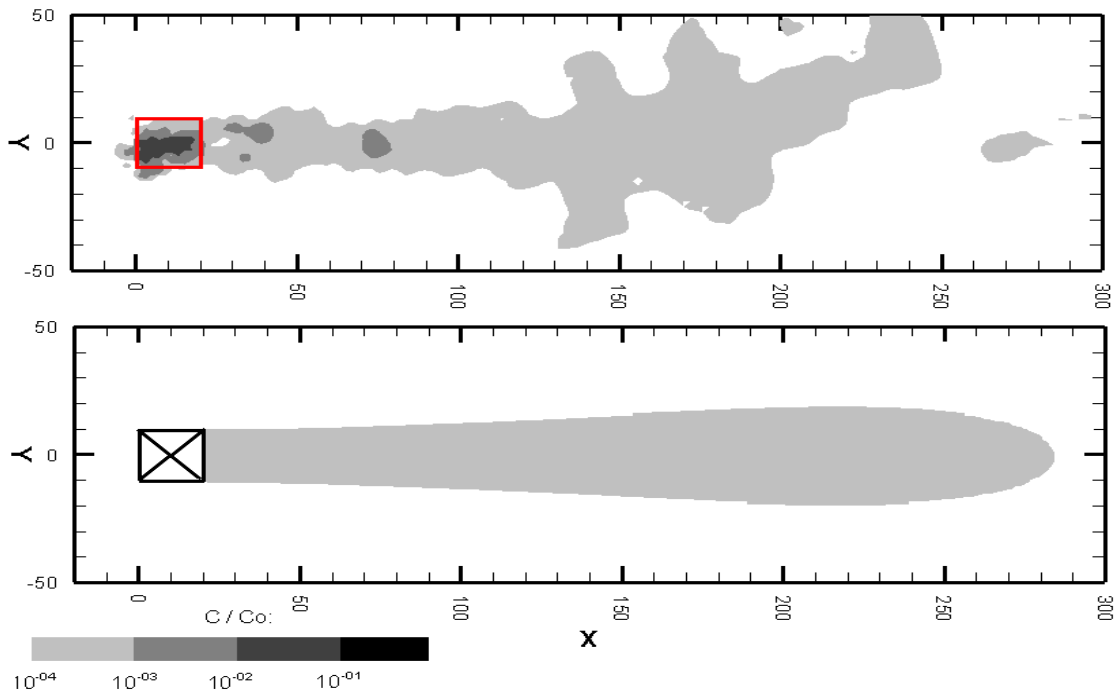


Figure 5.12. Results for 328 days.

5.3 Discussion

The goal of this study was to determine whether a screening-level analytical model could describe tritium transport at MADE-2. The site has been the subject of several previous studies, and a variety of modeling approaches have been used to simulate tritium transport at MADE-2. In one previous study of the MADE-2 tritium tracer test, Guan (2006) uses a dual-domain mass transfer model. The dual-domain mass transfer model (DDMT) divides the domain into two zones – a high permeability zone and a low permeability zone. The tracer is transported by advection and dispersion in the model. Mass transfer by diffusion occurs between the two zones, and is limited by the mass transfer rate term. Guan (2006) used a scale-dependent mass transfer term to simulate the tracer transport. The mass distributions calculated by Guan (2006) are shown in the right side of Figure 5.13.

Figure 5.13 compares the mass distributions simulated in REMChlor with the distributions calculated in Guan (2006). The mass distributions simulated in REMChlor use the values listed in Table 5.4 with an initial concentration of 40 pCi/mL. The mass distributions calculated by Guan (2006) use the dual-domain numerical model with variable mass transfer rates for each snapshot. The mass distributions calculated using REMChlor are similar to the distributions calculated using a dual-domain mass transfer model.

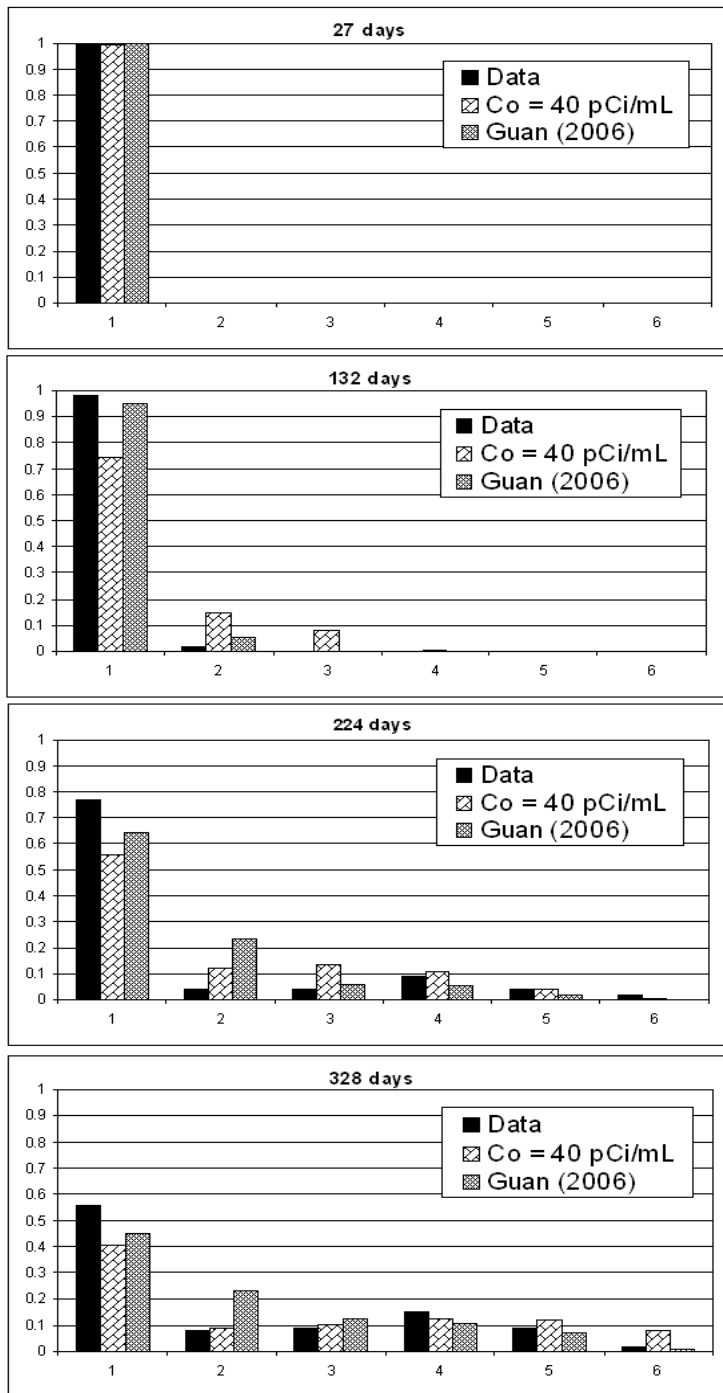


Figure 5.13. Comparison of mass distribution plots calculated using REMChlor and using a dual-domain mass transfer (DDMT) model. The mass distributions calculated in REMChlor are labeled $C_0 = 40$ pCi/mL. The distributions calculated using a DDMT model are taken from Guan (2006).

5.4 Implications

Remediation is often a goal at sites similar to MADE-2 where contaminants have been introduced to the aquifer. Many factors are considered to determine the best remediation method. The mass of the contaminant and the risk it poses to people and the environment exposed to the contaminant can play a big roll in determining what, if any, remediation should be done at the site. Many sites are monitored to see if the contaminant plume is stable or if it is shrinking or growing longer (McGuire et al., 2004).

At sites with a large degree of heterogeneity in the hydraulic conductivity field preferential flow paths can develop in the subsurface. Preferential flowpaths represent portions of the aquifer that dissolved solutes are preferentially transported through. Preferential flow paths can be large scale features of the aquifer or can be small scale (cm size or smaller) (Feehley et al., 2000).

For heterogeneous sites, the efficacy of a remediation scheme will be partially dependent on the rate of mass transfer from contaminant held in a low permeability zone back into the highly mobile zone (Guan 2006). In this study, the mass transfer is conceptualized by categorizing the aquifer into two zones – the source and the plume. The source is a reservoir for the contaminant that releases mass into the plume zone.

For MADE-2 the peak mass remains within the source zone for the one year duration of the experiment. At the end of the experiment (328 days) 56% of the injected mass was still in the 20-m long source zone. This suggests that the best strategy to reduce the total contaminant mass in the aquifer would be to remove mass in the source zone.

The possible effects of different remediation scenarios can be tested by using the remediation simulation features in REMChlor. Two hypothetical remediation techniques are considered. Remediation of the source zone and the plume zone are individually compared to the simulation where no remediation was performed.

The effect of source remediation can be considered by removing a percentage of the source mass in REMChlor. The scenario where 90% of the source mass is removed between the first and second year after the start of the experiment was considered.

Plume remediation can be considered in REMChlor by adjusting the solute decay rates in the plume zone. A hypothetical scenario where some method of remediation, such as pump and treat, is conducted at the site boundary is considered by dramatically increasing the decay rate at the boundary. For this scenario the boundary is defined to be at 300 m downgradient of the injection wells to correspond with the downgradient boundary of the sampling network. The decay rate was increased by nearly 4 orders of magnitude to simulate contaminant capture and removal between 300 and 310 m downgradient of the injection site. The plume remediation began at the end of the first year after the start of the experiment.

Figure 5.14 shows the concentrations down the centerline of the plume, where $y = 0$ m, for the no-remediation case and the source and plume remediation cases. The concentrations have been normalized to the tritium concentration of the injection solution. The no-remediation case shows that the concentration leaving the source zone (at $x = 0$ m) decreases each year while the length of the plume grows.

The case with source remediation, where 90% of the mass in the source zone was removed at the end of the first year (between 1 to 1.01 years), shows lower concentrations leaving the source zone than the no-remediation case. However the leading edges of the plumes strongly resemble those seen in the no-remediation case. This occurs because there is some mass already in the plume zone prior to the removal of the source mass.

The case with plume remediation shows the same concentrations entering the plume zone as the no-remediation case. It also shows a sharp drop in concentrations at 300 m after the first year. This is due to the dramatically increased decay rates between 300 and 310 m. This prevents a large amount of the mass from crossing the site boundary and traveling further downgradient. The increases in concentration downgradient of the site boundary for the second and third year are from the mass that crossed the site boundary prior to the increase in decay rates. For the plume remediation case the concentrations downgradient of the site boundary are much lower than in the no-remediation and source remediation case. This is because only a small amount of tritium had reached the site boundary at 300 m by the end of the first year. The plume remediation essentially cuts off the contaminant before it can leave the site boundary.

Many factors need to be considered before deciding the best remediation scheme at a site similar to MADE-2. If the ultimate goal was to reduce the total amount of mass in the system, then source remediation may be the best solution. However, if the goal is to limit the extent of the plume and reduce the travel distance then plume remediation would offer a better option. Also, the timeframe for implementing a remediation scheme

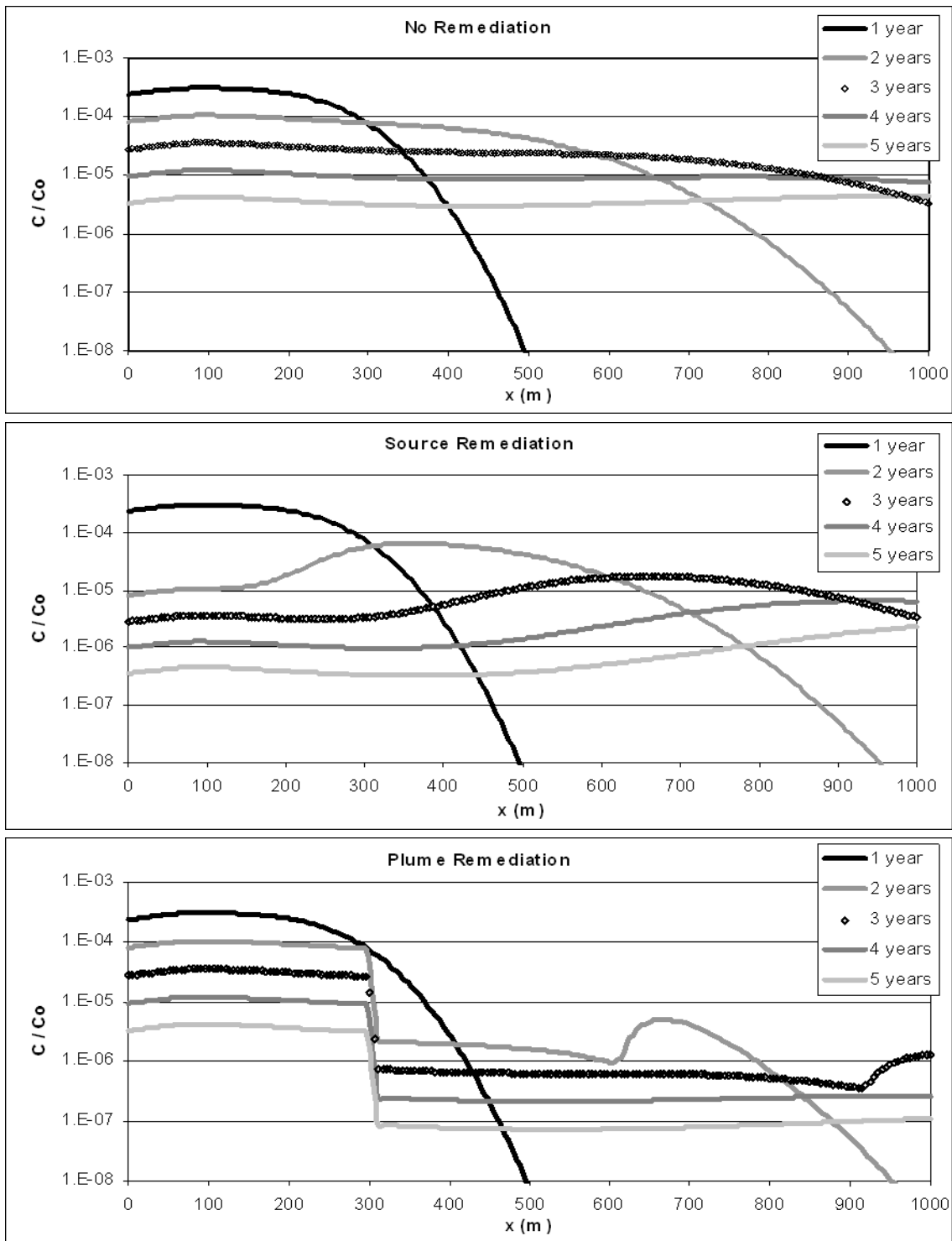


Figure 5.14. Concentrations along the centerline of the plume for the no-remediation case, and the source and plume remediation cases.

relative to the time contaminant was introduced to the aquifer will play a large role in determining the efficacy of the remediation approach.

CHAPTER 6 CONCLUSIONS

A screening – level groundwater transport model was applied to the tritium tracer experiment at MADE-2. The model used, REMChlor, was developed for sites with NAPL contamination. NAPL-contaminated sites typically have a source zone that acts as a reservoir of contaminant mass that is flushed downstream to create a plume zone. The tritium distributions observed during MADE-2 resemble the distributions seen at sites with NAPL contamination.

The goal of this study was to test whether the source-plume model used to conceptualize sites with NAPL is applicable to the tritium tracer test at MADE-2. The results show that REMChlor is successful at reproducing key features seen at the site. The simulation captures the length of the plume and reproduces the mass distributions reasonably well.

Several previous studies of the same data set have been conducted, with the general conclusion being that dual-domain mass transfer (DDMT) models are more suitable than traditional advection-dispersion models for the MADE site because of the highly heterogeneous hydraulic conductivity at the site. The dual-domain models are more complicated than the REMChlor model, but REMChlor was able to reproduce the key features seen during MADE-2 similarly to DDMT models. This is because the source zone in REMChlor behaves like mass transfer in DDMT models. The source zone acts as a reservoir of contaminant mass that is released into the plume zone, much like the immobile portion of a DDMT model releases mass into the mobile portion as time

increases. How the source zone is defined has a large impact on the simulation results from REMChlor.

Intuitively the source zone would seem to be the area immediately nearest to the injection wells. The observed tritium distributions from MADE-2 show that the highest concentrations stay within 20 m of the injection wells. Instead of defining the source zone as being the area immediate to the injection wells, the source was expanded to include the whole area that contains the peak concentrations. How the source zone is defined should be carefully considered. Observations, if available, should be used to interpret the source zone boundary.

At the MADE site the solute transport was controlled by the heterogeneous hydraulic conductivity field – the injected tracer was located in an area of low conductivity, and the conductivity heterogeneity leads to mechanisms like mass transfer and preferential flow paths. The heterogeneity at the MADE site lead to the presence of high tritium concentrations near the injection site, and a dilute tritium plume that extends downgradient of the injection site.

The REMChlor model was successful at describing the distributions of a conservative tracer at a site with a heterogeneous hydraulic conductivity field. This suggests that REMChlor may also be useful at other sites that have non NAPL contaminants. REMChlor could be used at sites that have a region of high concentration, similar to the source zone at MADE-2, and have a plume that develops downgradient from the source zone

REFERENCES

- Adams, E. E. and L. W. Gelhar (1992). "Field Study of Dispersion in a Heterogeneous Aquifer, 2. Spatial Moments Analysis." Water Resources Research **28**(12), 3293-3307.
- Amtec Engineering, I., Ed. (2003). Tecplot 10 User's Manual. Bellevue, Washington.
- Aziz, C. E., C. J. Newell and J. R. Gonzales (2002). BIOCHLOR Natural Attenuation Decision Support System Version 2.2 User's Manual Addendum, <http://www.epa.gov/ahaazvuc/download/models/biochlor22.pdf>.
- Aziz, C. E., C. J. Newell, J. R. Gonzales, P. Haas, T. P. Clement and Y. Sun (2000). BIOCHLOR natural attenuation decision support system User's Manual Version 1.1, U.S. EPA Office of Research and Development. **EPA/600/R-00/008**.
- Boggs, J. M., L. M. Beard and W. R. Waldrop (1993). Transport of tritium and four organic compounds during a natural-gradient experiment (MADE-2). Palo Alto, California, Electric Power Research Institute.
- Boggs, J. M., S. C. Young, L. M. Beard, L. W. Gelhar, K. R. Rehfeldt and E. E. Adams (1992). "Field Study of Dispersion in a Heterogeneous Aquifer 1. Overview and Site Description." Water Resources Research **28**(12), 3281-3291.
- Boggs, J. M., S. C. Young, D. J. Benton and Y. C. Chung (1990). Hydrogeologic Characterization of the MADE Site. Palo Alto, California, Electric Power Research Institute.
- Bowling, J. C., C. Zheng, A. B. Rodriguez and D. L. Harry (2006). "Geophysical constraints on contaminant transport modeling in a heterogeneous fluvial aquifer." Journal of Contaminant Hydrology **85**, 72-88.
- Domenico, P. A. (1987). "An analytical model for multidimensional transport of a decaying contaminant species." Journal of Hydrology **91**(1-2), 49-58.
- Eggleston, J. and S. Rojstaczer (1998). "Identification of large-scale hydraulic conductivity trends and the influence of trends on contaminant transport." Water Resources Research **34**(9), 2155-2168.
- Falta, R. W. (2008). "Methodology for Comparing Source and Plume Remediation Alternatives." Ground Water **46**(2), 272-285.

- Falta, R. W., N. Basu and P. S. Rao (2005). "Assessing impacts of partial mass depletion in DNAPL source zones: II. Coupling source strength functions to plume evolution." Journal of Contaminant Hydrology **79**, 45-46.
- Falta, R. W., P. S. Rao and N. Basu (2005). "Assessing the impacts of partial mass depletion in DNAPL source zones: I. Analytical modeling of source strength functions and plume response." Journal of Contaminant Hydrology **78**, 259-280.
- Falta, R. W., M. B. Stacy, A. Noman, M. Ahsanuzzaman, M. Wang and R. C. Earle (2007). REMChlor Remediation Evaluation Model for Chlorinated Solvents: User's Manual Beta Version 1.0.
- Feehley, C. E., C. Zheng and F. J. Molz (2000). "A dual-domain mass transfer approach for modeling solute transport in heterogeneous aquifers: Application to the Macrodispersion Experiment (MADE) site." Water Resources Research **36**(9), 2501-2515.
- Flach, G. P., S. A. Crisman and F. J. M. III (2004). "Comparison of Single-Domain and Dual-Domain Subsurface Transport Models." Ground Water **42**(6), 815-828.
- Guan, J. (2006). Analysis of a 3-D Tritium Transport Experiment at the MADE Site. Environmental Engineering and Science. Clemson, SC, Clemson University. **Ph. D.:** 92.
- Guan, J., F. J. Molz, Q. Zhou, H. H. Liu and C. Zheng (2008). "Behavior of the mass transfer coefficient during the MADE-2 experiment: New insights." Water Resources Research **44**(W02423, doi:10.1029/2007WR006120).
- Harvey, C. and S. M. Gorelick (2000). "Rate-limited mass transfer of macrodispersion: Which dominates plume evolution at the Macrodispersion Experiment (MADE) site?" Water Resources Research **36**(3), 637-650.
- McGuire, T. M., C. J. Newell, B. B. Looney, K. M. Vangelas and C. H. Sink (2004). "Historical Analysis of Monitored Natural Attenuation: A Survey of 191 Chlorinated Solvent Sites and 45 Solvent Plumes." Remediation Winter 2004, 99-112.
- Newell, C. J. and D. T. Adamson (2005). "Planning-Level Source Decay Models to Evaluate Impact of Source Depletion on Remediation Time Frame." Remediation Autumn, 27-47.
- Newell, C. J., R. K. McLeod and J. R. Gonzales (1996). BIOSCREEN Natural Attenuation Decision Support System User's Manual Version 1.3, U.S. EPA National Risk Management Research Laboratory. **EPA/600/R-96/087**.

- Parker, J. C. and E. Park (2004). "Modeling field-scale dense nonaqueous phase liquid dissolution kinetics in heterogeneous aquifers." Water Resources Research **40**, W05109.
- Rehfeldt, K. R., J. M. Boggs and L. W. Gelhar (1992). "Field Study of Dispersion in a Heterogeneous Aquifer 3. Geostatistical Analysis of Hydraulic Conductivity." Water Resources Research **28**(12), 3309-3324.
- USEPA. (2007). Tritium. Radiation Protection. Retrieved July 2008, from <http://www.epa.gov/rpdweb00/radionuclides/tritium.html>.
- USEPA. (2008). REMChlor. Center for Subsurface Modeling Support. Retrieved July 2008, from <http://www.epa.gov/ada/csamos/models/remchlor.html>.
- USNRC. (2007). Fact Sheet on Tritium, Radiation Protection Limits, and Drinking Water Standards. Retrieved July 2008, from <http://www.nrc.gov/reading-rm/doc-collections/fact-sheets/tritium-radiation-fs.html>.
- Wang, H. F. and M. P. Anderson (1982). Introduction to Groundwater Modeling: Finite Difference and Finite Element Methods. San Diego, CA, Academic Press.
- Zheng, C. and S. M. Gorelick (2003). "Analysis of Solute Transport in Flow Fields Influenced by Preferential Flowpaths at the Decimeter Scale." Ground Water **41**, 142-155.
- Zheng, C. and J. J. Jiao (1998). "Numerical Simulation of Tracer Tests in Heterogeneous Aquifer." Journal of Environmental Engineering **124**(6), 510-516.